

1988

## Advanced turbulence closure models and their application to buoyant and nonbuoyant flows

Mohamed Zaki Moustafa

*College of William and Mary - Virginia Institute of Marine Science*

Follow this and additional works at: <https://scholarworks.wm.edu/etd>



Part of the [Mechanical Engineering Commons](#)

---

### Recommended Citation

Moustafa, Mohamed Zaki, "Advanced turbulence closure models and their application to buoyant and nonbuoyant flows" (1988). *Dissertations, Theses, and Masters Projects*. William & Mary. Paper 1539616785.

<https://dx.doi.org/doi:10.25773/v5-r19t-gc67>

This Dissertation is brought to you for free and open access by the Theses, Dissertations, & Master Projects at W&M ScholarWorks. It has been accepted for inclusion in Dissertations, Theses, and Masters Projects by an authorized administrator of W&M ScholarWorks. For more information, please contact [scholarworks@wm.edu](mailto:scholarworks@wm.edu).

## INFORMATION TO USERS

The most advanced technology has been used to photograph and reproduce this manuscript from the microfilm master. UMI films the original text directly from the copy submitted. Thus, some dissertation copies are in typewriter face, while others may be from a computer printer.

In the unlikely event that the author did not send UMI a complete manuscript and there are missing pages, these will be noted. Also, if unauthorized copyrighted material had to be removed, a note will indicate the deletion.

Oversize materials (e.g., maps, drawings, charts) are reproduced by sectioning the original, beginning at the upper left-hand corner and continuing from left to right in equal sections with small overlaps. Each oversize page is available as one exposure on a standard 35 mm slide or as a 17" x 23" black and white photographic print for an additional charge.

Photographs included in the original manuscript have been reproduced xerographically in this copy. 35 mm slides or 6" x 9" black and white photographic prints are available for any photographs or illustrations appearing in this copy for an additional charge. Contact UMI directly to order.



Accessing the World's Information since 1938

300 North Zeeb Road, Ann Arbor, MI 48106-1346 USA



**Order Number 8827300**

**Advanced turbulence closure models and their application to  
buoyant and non-buoyant flows**

**Moustafa, Mohamed Zaki, Ph.D.**

**The College of William and Mary, 1988**

**Copyright ©1989 by Moustafa, Mohamed Zaki. All rights reserved.**

**U·M·I**  
300 N. Zeeb Rd.  
Ann Arbor, MI 48106



ADVANCED TURBULENCE CLOSURE MODELS AND THEIR  
APPLICATION TO BUOYANT AND NON-BUOYANT FLOWS

---

A Dissertation

Presented to

The Faculty of the School of Marine Science  
The College of William and Mary in Virginia

In Partial Fulfillment  
of the requirement for the Degree of  
Doctor of Philosophy

---

by

Mohamed Zaki Moustafa

1988

APPROVAL SHEET

This dissertation is submitted in partial fulfillment of the  
requirements for the degree of

Doctor of Philosophy

Mohamed Zaki Moustafa

Approved, March 1988

Carl F. Cerco

Carl F. Cerco, Chairman

Albert Y. Kuo

Albert Y. Kuo

Evon P. Ruzicki

Evon P. Ruzicki

John M. Brubaker

John M. Brubaker

John M. Hamrick

John Hamrick  
University of Virginia

William D. DuPaul

William D. DuPaul

©1989

Mohamed Zaki Moustafa

All Rights Reserved

## TURBULENCE CLOSURE MODELS

## ABSTRACT

In recent years, different approaches for modeling Reynolds stresses have been pursued by various authors. Two different closure schemes, representing two schools of thought, have been selected. The first closure scheme is the  $k-\epsilon$  model. The second closure scheme is the level two model. Each group has claimed that the proposed models are an improvement and an advancement over previous models employing the mixing length hypothesis as a closure scheme. Neither group however, has made thorough comparisons between the newly proposed schemes and the most commonly used approach the mixing length hypothesis.

The main objective of this paper is to test the applicability of the standard  $k-\epsilon$  and the level two models in buoyant and non-buoyant flows. In addition, comparisons have been made between these new closure schemes and an existing mixing length model.

Results obtained by employing the level two model for buoyant and non-buoyant flows are considered to be an improvement over those obtained by employing the mixing length model. A single set of constants was used for all level two model applications. Unlike the mixing-length closure scheme which requires tuning of the constants employed by the model for each individual application, there was no further tuning required for the level two model.

Comparison between model results have shown no substantial improvement of the  $k-\epsilon$  model over the level two model.

## TABLE OF CONTENTS

	Page
ACKNOWLEDGEMENTS.....	iv
LIST OF TABLES.....	v
LIST OF FIGURES.....	vi
ABSTRACT.....	viii
CHAPTER I. INTRODUCTION.....	2
CHAPTER II. GOVERNING EQUATIONS AND TURBULENCE CLOSURE MODELS.....	6
CHAPTER III. FINITE DIFFERENCE FORM FOR THE $k-\epsilon$ MODEL.....	35
CHAPTER IV. VERIFICATION AND APPLICATIONS OF THE $k-\epsilon$ MODEL.....	45
CHAPTER V. VERIFICATION AND APPLICATIONS OF THE LEVEL TWO MODEL.....	75
CHAPTER VI. SUMMARY, CONCLUSIONS AND SUGGESTIONS FOR FUTURE WORK.....	94
BIBLIOGRAPHY.....	100
VITA.....	108

#### ACKNOWLEDGEMENTS

The author wishes to express appreciation to his major professor, Dr. Carl F. Cerco, for his patient guidance and encouragement during the course of this study. Thanks and appreciation are also extended to Dr. Albert Y. Kuo, Dr. Evon P. Ruzicki, Dr. John Brubaker, Dr W. D. DuPaul and Dr. John Hamrick for their criticism of the manuscript. Special thanks go to Dr. Bruce Neilson for his encouragement. Finally, I am most indebted to my wife, Mary Sue Moustafa, for many hours of reading and correcting my English grammar. Last but not least, thanks for the greatest typist helper, Ms. Barbara Cauthorn. Special thanks goes to Pamela Mason for all the time she invested helping me with my English.

LIST OF TABLES

TABLE		Page
4-I	Eddy Viscosity Estimates By Method A and B.....	62
4-II	Estimates of Energy and Its Dissipation By Method A and B.....	62
4-III	Estimates of Eddy Viscosity, Energy and Its Dissipation by Method A.....	62
5-II	Estimates of Eddy Viscosity, Energy and Its Dissipation by Level Two and Mixing Length Models.....	86

## LIST OF FIGURES

FIGURE	Page
3.1. Finite difference grid and axis orientation.....	44
4.1. Velocity contours in an open channel; friction forces are not included method A.....	63
4.2. Velocity contours in an open channel; friction forces are not included method B.....	64
4.3. Velocity contours in an open channel; friction forces are included method A.....	65
4.4. Velocity contours in an open channel; friction forces are included method B.....	66
4.5. Velocity overshoot near a rough bottom method A.....	67
4.6. Velocity overshoot near a rough bottom method B.....	68
4.7. Instantaneous eddy viscosity profiles at different times within one tidal cycle at a specific location method A .....	69
4.8. Instantaneous eddy viscosity profiles at different times within one tidal cycle at a specific location method A .....	70
4.9. Tidal-averaged eddy viscosity profiles at different locations along the channel method A.....	71

4.10. Tidal-averaged eddy viscosity profiles at different locations along the channel method B.....	72
4.11. Tidal-averaged energy concentration profiles at different locations along the channel method A.....	73
4.12. Tidal-averaged energy concentration profiles at different locations along the channel method B.....	74
5.1. Velocity contours in an open channel; friction forces are not included level two model.....	87
5.2. Velocity contours in an open channel; friction forces are included level two model.....	88
5.3. Calibration of laboratory bottom roughness level two model.....	89
5.4. Level two model predictions and flume data of longitudinal salinity distributions and mixing length model Predictions.....	90
5.5. Flume tidal-averaged vertical salinity distributions along with the mixing length and level two model predictions.....	91
5.6. Flume tidal-averaged horizontal velocities along with the mixing length and level two model Predictions.....	92
5.7. Tidal-averaged vertical velocities distributions; flume, mixing length and level two model.....	93

## ABSTRACT

In recent years, different approaches for modeling Reynolds stresses have been pursued by various authors. Two different closure schemes, representing two schools of thought, have been selected. The first closure scheme is the  $k-\epsilon$  model. The second closure scheme is the level two model. Each group has claimed that the proposed models are an improvement and an advancement over previous models employing the mixing length hypothesis as a closure scheme. Neither group however, has made thorough comparisons between the newly proposed schemes and the most commonly used approach the mixing length hypothesis.

The standard  $k-\epsilon$  model requires the solution of two partial differential equations to determine Reynolds stresses and hence close the set of equations that govern the mean flow. The first equation solves for turbulent kinetic energy,  $k$ , while the second solves for its dissipation rate,  $\epsilon$ . The closure is then accomplished by a simple relationship as was first suggested by Rodi (1980a).

Unlike the  $k-\epsilon$  model, the level two model does not require the solution of additional equations. Instead, Reynolds stresses are calculated by a simple algebraic expression. The level two model can be considered a mixing-length hypothesis closure scheme modified by a stability function.

The main objective of this paper is to test the applicability of the standard  $k-\epsilon$  and the level two models in buoyant and non-buoyant flows. In addition, comparisons have been made between these new closure schemes and an existing mixing length model. Reasonable agreement was obtained between model results and the analytical solution for a nonbuoyant open channel flow when employing the  $k-\epsilon$  model. Better results were achieved by adjusting the constant,  $C_\mu$ , proposed by Rodi (1980a) in the eddy viscosity relationship.

As a second test, the model was applied to a continuously stratified open channel flow. Difficulties encountered during the second application are identified. Reasons for the problems are discussed and suggestions are made to overcome the shortcomings.

Results obtained by employing the level two model for buoyant and non-buoyant flows are considered to be an improvement over those obtained by employing the mixing length model. A single set of constants was used for all level two model applications. Unlike the mixing-length closure scheme which requires tuning of the constants employed by the model for each individual application, there was no further tuning required for the level two model. Additionally, the consistent results obtained by the level two model are considered an improvement over the mixing-length model when compared with flume data collected under stratified conditions.

Comparison between model results have shown no substantial improvement of the  $k-\epsilon$  model over the level two model for non-buoyant channel flow. The  $k-\epsilon$  model requires far more computer time than the level two model for the same test run. The level two model is simpler and easier to apply than the  $k-\epsilon$  model. Since no model run can be made employing the  $k-\epsilon$  model as a closure scheme for buoyant flows, no comparison can be made between the two closure schemes under this flow condition.

## DEDICATION

This work is dedicated to my parents, Zaki and Samiah Moustafa who loved, encouraged and cared for me all my entire life.

**ADVANCED TURBULENCE CLOSURE MODELS AND THEIR  
APPLICATION TO BUOYANT AND NON-BUOYANT FLOWS**

## CHAPTER I.

### INTRODUCTION

Turbulent motion is characterized as unsteady, highly random, and strongly three dimensional. A more precise definition is: "Turbulent fluid motion is an irregular condition of flow in which the various quantities show a random variation with time and space, so that statistically distinct average values can be discerned" (Hinze, 1959). The state of turbulent mixing motion is responsible not only for an exchange of momentum, but also for enhancing the transfer of heat and mass in fields of flow associated with non-uniform distributions of temperature or concentration.

Estuaries present one of the greatest challenges to environmental scientists. The complicated nature of different forcing functions (e.g. tides, wind, fresh-water etc.) continuously acting on fluid in an irregular channel results in turbulent flow. Because of its complicated nature, it is unlikely that scientists will achieve a complete understanding of the mechanism of turbulence, yet, it is their task to predict velocity and transport of heat and mass phenomena existing in the natural environment.

Due to oscillating, unsteady non-uniform flows, estuaries are among systems for which transport and history effects of turbulence are not

adequately accounted for by a mixing length model (Smith and Takhar, 1981). For example, model simulations show that low velocity gradients (i.e. near slack water) result in low eddy viscosity (Leonard, 1977) also, a velocity reversal implies a zero eddy viscosity (Blumberg, 1975) both are not observed in prototypes. In addition, the length scale, required by the mixing length hypothesis, is difficult to define in more complex flows (Rodi, 1980a).

Predicting flow behaviour in a turbulent environment by way of laboratory and field experiments is tedious, time-consuming and very expensive. On the other hand, prediction by the way of computational methods, once formulated, is easier to apply and more economical. Thus, most scientists and engineers prefer the second approach.

#### A. Mean-flow equations and the problem of closure

In order to accurately compute the turbulent transport process at all points in time and space, the complete Navier-Stokes equations should be solved. There exists no general solution for the exact equations. Thus, to arrive at a computationally tractable configuration, approximations must be introduced for the turbulence correlations in the form of model assumptions. Predictions of turbulent flow fields, temperature and concentration, developed so far have been based on empirical or semi-empirical hypotheses.

In order to establish a turbulence model, a relationship between the Reynolds stresses, produced by the mixing motion and the mean values of the velocity components, should be established as well as a suitable hypothesis concerning heat and mass transfer. In other words, a turbulence model should relate turbulent transport quantities to the

values of mean flow. A turbulence model can be defined as a set of equations from which turbulent transport terms can be determined and thus close the system governing the mean-flow. Turbulence models simulate the effect of turbulent processes on the mean-flow behaviour. Since they are not the exact equations, turbulence models require empirical input in the form of constants or functions.

Because the Navier-Stokes equations at present, can not be solved for turbulent flows and since we are not interested in the details of fluctuating motion, a statistical approach is taken. The instantaneous variables are decomposed into two terms: a mean variable and a departure from that mean. In practical application, the mean variables could be the average values over appropriate temporal and/or spatial domains. Taking the average produces the equations governing the mean variables. The time period (or spatial domain) of average should be longer (or larger) than the turbulent fluctuations and shorter than the time (or spatial) scale of mean flow. The resulting equations describe the distribution of mean velocity, temperature, and species concentration in the flow and thus the quantities of prime interest. Unfortunately, the averaging process creates a new problem. The equations no longer define a closed system since they contain unknown correlation terms representing the transport of mean momentum (Reynolds stress), and heat or mass (Reynolds flux) transport via turbulent motion. The closure for these equations can only be achieved by empirical formula or by a turbulence model.

## B. Intent of this investigation

The intent of this investigation is to employ two different closure schemes, k- $\epsilon$  and level two models. Application and comparisons will be made between the two selected schemes and an existing mixing-length model using the analytical solution for open channel flow as a first test. As a second test, these schemes will be applied to a continuously stratified open channel flow. Results obtained from the previous tests will be compared and discussed.

A number of estuary models exist (Cerco, 1982), most of which use mixing-length hypothesis to calculate eddy viscosity and thus, require empirical constants. The standard k- $\epsilon$  model does not require tuning of all constants employed in the model for each individual application. The k- $\epsilon$  model should also provide more realistic results as suggested by Rodi (1980a). On the other hand, the level two model requires several empirical constants to determine the stability function (Mellor and Yamada, 1982). These constants can be deduced from neutral conditions.

This investigation intends to answer the following questions:

- 1- Are the proposed models, k- $\epsilon$  or level two, easier to apply than a mixing-length model ?
- 2- Do the proposed models provide more realistic results than a mixing-length model ?
- 3- Are results improved, if so are the models worthwhile pursuing ?

To answer these questions, the k- $\epsilon$  and level two models will be compared with an existing mixing-length-model. Agreement between the models with analytical solutions, and with experimental data will be examined. Computation time for all models will be noted as one benchmark of performance.

## CHAPTER II.

### GOVERNING EQUATIONS AND TURBULENCE

#### CLOSURE MODELS

##### A. Mean-flow equations and the problem of closure

The well established set of differential equations which describes the dynamics of an estuary are: the momentum balance equation, the continuity equation, the conservation of salt equation, and the equation of state. For an incompressible flow, in a rotating coordinate system, such as the earth, and by employing the Boussinesq approximation, these equations can be expressed in tensor notation as

momentum conservation

$$\frac{\partial u_i}{\partial t} + u_j \frac{\partial u_i}{\partial x_j} + 2 \xi_{ijk} \Omega_j u_k = - \frac{1}{\rho_0} \frac{\partial p}{\partial x_i} + \nu \frac{\partial^2 u_i}{\partial x_j \partial x_j} + g_i \frac{\Delta \rho}{\rho} \quad (2-1)$$

mass conservation: continuity equation

$$\frac{\partial u_i}{\partial x_i} = 0 \quad (2-2)$$

salt conservation:

$$\frac{\partial s}{\partial t} + \frac{\partial}{\partial x_i} (u_i s) = D \frac{\partial^2 s}{\partial x_i \partial x_i} \quad (2-3)$$

equation of state

$$\rho = \rho_0 (1. + \alpha T + \beta s) \quad (2-4)$$

in which

- $x_i$  = Cartesian space coordinate
- $u_i$  = instantaneous component of velocity in direction  $x_i$
- $\nu$  = kinematic viscosity
- $\rho_0$  = reference density, a constant
- $\rho$  = density
- $\Delta\rho$  =  $(\rho - \rho_0)$
- $t$  = time
- $s$  = salinity
- $T$  = temperature
- $p$  = pressure
- $\alpha, \beta$  = empirical constants
- $g_i$  = acceleration due to gravity
- $D$  = molecular diffusion coefficient
- $\Omega$  = angular velocity of the earth's rotation
- $\xi_{ijk}$  = alternating isotropic tensor
  - = +1 if i, j, k are in cyclic order
  - = -1 if i, j, k are in anticyclic order
  - = 0 if any two indices are repeated

Coefficients  $\alpha$  and  $\beta$  of equation (2-4) are functions of temperature. The density of sea water depends on both the salinity and temperature, but in estuaries the salinity range (spatial gradient) is large and temperature range is generally small. Consequently temperature has a relatively small influence on the density and may be ignored. Furthermore, for a narrow body of water such as an estuarine

river, the effect of the earth's rotation in the momentum equation can also be neglected. By introducing the preceding considerations, equations (2-1 to 2-4) can be simplified. The resulting equations, however, cannot at present be solved for the turbulent flows of main interest i.e. flow in estuaries. In order to simplify and reach a solvable set of equations, Reynolds (cited from Schlichting, 1968) decomposed the instantaneous variables into a mean variable and a departure from that mean. Thus

$$\begin{aligned} u_i &= U_i + u_i' \\ p &= P + p' \\ s &= S + s' \end{aligned} \quad (2-5)$$

In which

$U_i, P, S$  = means of velocity, pressure, salinity and  
 $u_i', p', s'$  = departures from those means

Substituting equations 2-5 into 2-1 to 2-4 and taking the average produces the equations governing the mean variables. The time period (and/or spatial domain) of averaging, as mentioned in chapter 1, should be longer than the time (or spatial) scale of turbulent fluctuations and shorter than the time (or spatial) scale of mean flow (e.g tidal period in estuaries). The application of Reynolds rules of averaging results in

$$\frac{\partial U_i}{\partial t} + U_j \frac{\partial U_i}{\partial x_j} = - \frac{1}{\rho_0} \frac{\partial P}{\partial x_i} - \frac{\partial}{\partial x_j} \overline{(u_i' u_j')} + g_i \left( \frac{\Delta \rho}{\rho_0} \right) \quad (2-6)$$

$$\frac{\partial U_i}{\partial x_i} = 0 \quad (2-7)$$

$$\frac{\partial S}{\partial t} + \frac{\partial}{\partial x_i} (U_i S) = - \frac{\partial}{\partial x_i} \overline{(u_i' s')} \quad (2-8)$$

$$\rho = \rho_0 (1.0 + \beta S) \quad (2-9)$$

In most flow regions, the turbulent stresses  $\overline{u_i u_j}$  and fluxes  $\overline{u_i s}$  are much larger than their molecular counterparts which are therefore neglected in equations (2-6) and (2-8).

The above set contains the equations governing the mean-flow variables. They no longer form a closed set due to the presence of the turbulent stresses and fluxes. These equations (2-6 to 2-9), contain more unknowns than the equations available to solve them.

The system of equations can only be solved if turbulence correlations  $\overline{u_i u_j}$  and  $\overline{u_i s}$  can be determined. In fact, the determination of these correlations, or the closure scheme, is the main problem in calculating turbulent flows. Since the solution of exact equations can not be carried out in practice at the present time, all closure techniques have been developed using approximations.

## B. Classification of turbulence models

There exist two ways to classify turbulent closure models. The most commonly used scheme for classifying turbulence models is according to how many equations are used for closure (Rodi, 1980a). The second approach is dependent on the complexity of the closure scheme and the ordering of terms appearing in Reynolds stress equations (Mellor and Yamada, 1982). Rodi's classification is adopted herein with reference to Mellor and Yamada's classification when appropriate.

### B-1 Zero-equation models

The simplest method to solve the closure problem is to replace or approximate Reynolds stresses and fluxes directly. This technique leads to Boussinesq's eddy viscosity concept and Prandtl's mixing length

hypothesis (cited from Schlichting, 1968). Boussinesq assumed that: analogous to the viscous stresses in laminar flow, 'turbulent' or Reynolds stresses are proportional to the mean velocity gradient and may be expressed (Hinze, 1959) as

$$-\overline{u_i u_j} = \nu_t \left( \frac{\partial \overline{u_i}}{\partial x_j} + \frac{\partial \overline{u_j}}{\partial x_i} \right) - \frac{2}{3} k \delta_{ij} \quad (2-10)$$

Turbulent heat or mass transport is assumed to be related to the gradient of the transported quantity

$$-\overline{u_i s} = \Gamma \frac{\partial \overline{s}}{\partial x_i} \quad (2-11)$$

in which

$\delta_{ij}$  = the Kronecker delta ( $\delta_{ij} = 0$  for  $i \neq j$  and  $\delta_{ij} = 1$  for  $i = j$ )

$\nu_t$  = the turbulent, or eddy viscosity

$k$  = turbulent kinetic energy per unit mass

$\Gamma$  = the turbulent diffusivity of salt

The Reynolds analogy between momentum and mass transport suggest that  $\Gamma$  is closely related to  $\nu_t$

$$\sigma_t = \frac{\nu_t}{\Gamma} \quad (2-12)$$

where  $\sigma_t$  is the turbulent Schmidt number.

One can see that the problem of closure has been shifted towards the determination of the eddy viscosity. The Boussinesq assumption has the great disadvantage that eddy viscosity is not a fluid property but depends on the state of turbulence. The eddy viscosity concept offers no solution to describe this dependency.

Two points have to be addressed before proceeding any further. First of all, the term involving the Kronecker delta in equation 2-10 is added to ensure that the sum of normal stresses is twice the kinetic

energy (Rodi, 1980a). When  $i$  equals  $j$  and sums over 1, 2 and 3 in equation 2-10, the first term on the right hand side becomes zero by continuity leaving us with normal stresses. These normal stresses act as pressure terms but do not need to be determined since they are much smaller than the pressure term in equation 2-6. The second point pertains to Reynolds analogy which assumes that the magnitude of turbulent eddy viscosity and turbulent eddy diffusivity are always the same. According to this assumption, the Schmidt number in equation 2-12 is defined as unity. Launder (1976) reported that a Schmidt number of 0.7 is a reasonable value to be used for inhomogeneous free shear flows. On the other hand, Jobson and Sayre (1970), in a study of an open channel turbulent shear flow, reported that the Schmidt number is equal to unity thus making Reynolds assumption valid. In estuaries however, vertical shear predominates, as it does in open channel flow. Therefore, a Schmidt number of 1.0 will be adopted for this study.

#### B-1-1 Constant eddy viscosity

Since the Boussinesq assumption has offered no relation to describe the dependency of  $\nu_t$  on turbulence, a constant value for  $\nu_t$  has been employed as a direct approximation for Reynolds stress (Pritchard, 1956; Hansen and Rattray, 1963; Feata and Hansen, 1976). It is apparent that the constant eddy viscosity assumption has failed to consider the variation in  $\nu_t$  with respect to space and time. A constant  $\nu_t$ , however, in some cases has been successfully applied to obtain results at a first order approximation (Le Mehaute, 1976). On the other hand, a constant value for  $\nu_t$  did not accurately reproduce the observed vertical velocity

and salinity profiles in estuaries (Howden and Hamilton, 1975; Elliot, 1976; Hamilton, 1975; Wang and Kravitz, 1980).

The use of a constant eddy viscosity has failed to gain popularity in the field of hydraulics because of its limited range of application (Rodi, 1980a; Reynolds, 1974). For example, in a fully developed open channel flow, eddy viscosity has an almost parabolic distribution with depth (Schlichting, 1968). Therefore, a constant eddy viscosity will predict an unrealistic distribution for vertical turbulent transport processes. The limited applicability of a constant eddy viscosity has led workers to discard this approach and seek other techniques.

#### B-1-2 Mixing-length model

In order to improve the preceding method, it is necessary to find an empirical relation between the eddy viscosity  $\nu_t$  and the mean velocity. Prandtl made an important advance in this direction. In his Mixing Length hypothesis, Prandtl assumed that  $\nu_t$  was proportional to a characteristic fluctuating velocity  $V'$  and a characteristic length scale  $L$ .

$$\nu_t = V' \cdot L \quad (2-13)$$

In two-dimensional channel flow with flow direction parallel to the  $x$ -axis and the  $y$ -axis is directed upward,  $V'$  is related to the mean velocity,  $U$ , by

$$V' = L \frac{\partial U}{\partial y} \quad (2-14)$$

Substituting equation 2-14 in 2-13 results in

$$\nu_t = A L^2 \frac{\partial U}{\partial y} \quad (2-15)$$

in which

A = an empirical constant

It should be noted that the constant, A, in the above equation can now be included with the unknown mixing length, L. One can also observe that  $\nu_t$ , will in general, be a function of position and time. For general flows, the mixing length hypothesis may be written as follows (Rodi, 1980a)

$$\nu_t = L^2 \left[ -\frac{\partial U_i}{\partial x_j} \left( \frac{\partial U_i}{\partial x_j} + \frac{\partial U_j}{\partial x_i} \right) \right]^{\frac{1}{2}} \quad (2-16)$$

Equation (2-16) can now be introduced into equation 2-10 in order to account for all Reynolds stress components. The mixing length hypothesis relates the eddy viscosity to the local mean-velocity gradient and mathematically describes this relationship. Prandtl's hypothesis introduces a new unknown, L, which must be determined. The characteristic length scale is not a fluid property but, as the eddy viscosity, depends on the state of turbulence and the geometry of the flow. Thus, any expression that describes L must account for all these effects. Various formulae are available to approximate the length scale. Most length scale formulae reported in the literature were experimentally obtained. The first approximation is purely empirical and only valid for special cases (Le Mehaute, 1976). For example, against the wall of a pipe, L is assumed to be linearly related to the distance Y from the wall as follows

$$L = a Y \quad (2-17)$$

in which

a = empirical constant

Von Karman developed an expression which determines L independent of flow type (cited from Launder and Spalding, 1972 ; Bradshaw, 1972).

He assumed that  $L$  is the ratio of the first to the second derivative of the mean velocity. In a well developed channel flow, a maximum velocity occurs at some distance from the bottom boundary. According to Von Karman's similarity hypothesis,  $\nu_t$  is zero at this location. To avoid such a discrepancy, Prandtl proposed a different formula to determine  $L$ . His formula was soon discarded because of its complicated nature and due to the disagreement between observed and predicted values away from the wall (Launder and Spalding, 1972).

Stratification also has a pronounced effect on the mixing length. The presence of stable stratification tends to reduce the size of the characteristic mixing length. Therefore, in order to remove these deficiencies, investigators have suggested various modifications. One such modification is to include a stratification parameter (e.g. Richardson number) to account for buoyancy effects in a nonhomogeneous flow (Kent, et al., 1959; Pritchard, 1960; Bradshaw, 1972). Another improvement is to add an extra term to the eddy viscosity formula to account for turbulence whenever a zero velocity gradient exists (Bowden and Hamilton, 1976).

Models using the mixing length hypothesis require empirical inputs which have to be determined for each turbulent flow case. This is one of the major drawbacks of the mixing length model. A second disadvantage is that mixing length theory assumes a state of local equilibrium, i.e. the production of energy is equal to its dissipation, (Rodi, 1980a). According to Mellor and Yamada's classification, this type of closure is equivalent to the level two model.

The mixing length model has the advantage of being simple, yet it requires a prior theoretical knowledge, which is not always available.

to determine the characteristic mixing length,  $L$ . Despite this shortcoming, investigators prefer to use the mixing length hypothesis because of its simplicity. On the other hand, Bradshaw (1972), has claimed that the main reason for the success of mixing length and eddy viscosity theories is attributed to the fact that they were tested against simple flow cases in which the flow was in state of local equilibrium (production of energy is equal to dissipation). Although estuaries are not in a state of local equilibrium, a modified version of the mixing length formula has been shown to obtain reasonable results when applied to estuaries (Cerco, 1982; Rodi, 1980a; Blumberg, 1977; Bowden and Hamilton, 1976).

The modified version of mixing length formulation employs several empirical constants which have to be determined for individual cases. More complex and advanced models were developed in order to overcome these limitations. In addition, various workers have concluded that better results may only be obtained through methods that employ transport equations (Rodi, 1980a and 1980b; Bradshaw, 1972; Launder and Spalding, 1972).

### **B-1-3 Level-two model**

According to Mellor and Yamada (1974) the level two model is equivalent to an eddy viscosity concept. This model assumes local equilibrium to prevail (i.e. production and dissipation of energy are in balance). This means that turbulence dissipates at the same rate it is being generated. As will be seen shortly, the level two model is an eddy viscosity concept modified by a stability function. If the boundary layer approximation is introduced to the level two model, i.e.

the vertical component of the momentum equation becomes hydrostatic and all components of the tensor  $\frac{\partial U_i}{\partial x_j}$  may be neglected except for  $\frac{\partial U}{\partial z}$ , then according to Mellor and Yamada (1982) the level two model can be written as follows:

$$-\frac{g}{l} = -\overline{u'w'} - \beta \overline{g'w'} \quad (2-18)$$

$$-\overline{u'w'} = K_m \frac{\partial U}{\partial z} \quad (2-18a)$$

$$-\overline{w's'} = K_h \frac{\partial S}{\partial z} \quad (2-18b)$$

Substituting equations (2-18a) and (2-18b) into equation (2-18) results in

$$-\frac{g}{l} = K_m \left( \frac{\partial U}{\partial z} \right)^2 + K_h \beta \overline{g'w'} \frac{\partial S}{\partial z} \quad (2-18c)$$

in which

$$K_m = L q S_m = \text{momentum eddy coefficient} \quad (2-18d)$$

$$K_h = L q S_h = \text{mass eddy coefficient} \quad (2-18e)$$

$$q^2 = \overline{u_i'^2} = \text{twice of turbulent kinetic energy per unit mass}$$

$$l = B_1 L$$

$$L = \text{master length scale}$$

$S_m$  and  $S_h$  are the stability functions and depend on flux

Richardson number ( $R_f$ ). These functions are defined as follows :

$$S_m = \frac{A_1}{A_2} \frac{B_1(\gamma_1 - C_1) - [B_1(\gamma_1 - C_1) + 6(A_1 + 3A_2)] R_f}{B_1\gamma_1 - [B_1(\gamma_1 + \gamma_2) - 3A_1] R_f} S_h$$

$$S_h = 3A_2 \frac{\gamma_1 - (\gamma_1 + \gamma_2) R_f}{1 - R_f}$$

in which

$$\gamma_1 = \frac{1}{3} - \left( 2 \frac{A_1}{B_1} \right)$$

$$\gamma_2 = \left( -\frac{R_1}{B_1} \right) + \left( 6 \frac{A_1}{B_1} \right)$$

$$R_f = - \frac{g \beta K_h \frac{\partial S}{\partial z}}{K_m \left( \frac{\partial U}{\partial z} \right) \left( \frac{\partial U}{\partial z} \right)}$$

$$R_i = - \frac{g \beta \frac{\partial S}{\partial z}}{\left( \frac{\partial U}{\partial z} \right) \left( \frac{\partial U}{\partial z} \right)}$$

$$A = B_1' S_m^{1.5}$$

$$b = B_2' S_h S_m^{1.5}$$

$A_1, B_1, A_2, C_1$  = empirical constants

Substituting equations (2-18d) and (2-18e) into equation (2-18c) as well as the defined quantities  $R_i$  and  $R_f$  it can be shown that

$$K_m = A L^2 \frac{\partial U}{\partial z} (1 - R_f) \quad (2-19)$$

$$K_h = b L^2 \frac{\partial U}{\partial z} (1 - R_f) \quad (2-20)$$

Equations (2-19) and (2-20) are similar to equation (2-15). The only difference is that this equation is modified by a flux Richardson number. For neutral conditions,  $R_f$  is equal to zero and equations (2-19) and (2-20) are reduced to the mixing length hypothesis. One can now see that the level two model is essentially an eddy viscosity concept with the stratification effect included via the stability function. The stability function is an algebraic expression and can be found in Mellor and Yamada (1974, 1982). Constants needed for this function can be deduced from turbulent measurements made in the absence of buoyant forces. Once obtained, no further adjustment is required (Mellor and Yamada, 1982). As for the length scale they argued that most valid prescribed formulae will perform adequately.

Alternatively, these authors have shown that the level two model can also be expressed in terms of mean flow quantities rather than turbulent quantities. Therefore, in a more traditional approach, i.e.

mixing length format, the level two model can be expressed as (Mellor and Yamada, 1974):

$$\overline{-u'w'} = L^2 S_m \left( \frac{\partial U}{\partial z} \right)^2 \quad (2-21)$$

$$\overline{-w's'} = L^2 S_h \left( \frac{\partial U}{\partial z} \right) \left( \frac{\partial S}{\partial z} \right) \quad (2-22)$$

in which

$$S_m = B_1^{-1} \left( \bar{S}_m \right)^{1.2} (1 - R_f)^{1.2}$$

$$S_h = B_1^{-1} \bar{S}_h \left( \bar{S}_m \right)^{1.2} (1 - R_f)^{1.2}$$

where

$$\bar{S}_m = 3A_1 \frac{\gamma_1 - C_1 - (6A_1 + 3A_2) / B_1}{\gamma_1 - \gamma_2 + (3A_1 / B_1)} (\gamma_1 - \gamma_2)$$

$$\bar{S}_h = 3A_2 (\gamma_1 - \gamma_2)$$

Mellor and Yamada (1974) have introduced a turbulence closure scheme labelled as level one model. This model is not substantially different from their level two model. The main difference between the two models are the stability function and the critical Richardson flux number at which mixing ceases.

## B-2 One-equation model

In an eddy viscosity-diffusivity model, transport and history effects of turbulence can be accounted for by solving a transport equation for a suitable parameter which characterizes the turbulence. The turbulent kinetic energy per unit mass,  $k$ , is such a parameter in that it characterizes the intensity of the fluctuating motion. Turbulent kinetic energy is contained mainly in large-scale fluctuations. The square root of  $k$  is the velocity scale for this motion. An exact equation describing the dynamics of turbulence kinetic energy,  $k$ , can be derived from the Navier-Stokes equations by simple

manipulations (Hinze, 1959). The  $k$  equation contains a higher order correlation, as will be seen in a later chapter. As a result, assumptions have to be introduced to model these terms.

One-equation models account for transport and history effects on the turbulent kinetic energy but not for the mixing length. Therefore, these models have offered no additional improvement with regard to the characteristic length scale. On the other hand, these models allow energy generated at a point to be transported elsewhere. Thus, these models appear to be superior to models using the mixing-length hypothesis (Launder and Spalding, 1972).

While Prandtl's concept is a physically attractive simple idea, it is only capable of describing very simple flows to a useful level of approximation. Due to the shortcomings of the mixing length hypothesis, a new and more suitable velocity scale was favoured over the mean velocity gradient employed in zero-equation models. The new characteristic velocity scale,  $k^{1/2}$ , is defined by Rodi (1980a) as

$$k = \frac{1}{2} ( u_1^2 + v_1^2 + w_1^2 ) \quad (2-23)$$

Substituting this velocity scale in equation (2-13) leads to

$$\nu_t = C_\mu^* \frac{\nu^2}{k^{1/2}} L \quad (2-24)$$

In which

$C_\mu^*$  = an empirical constant

This expression is generally known as the Kolmogorov-Prandtl expression. Prandtl, (1925) suggested solving a transport equation to determine the distribution of  $k$ . In order to calculate the turbulent eddy viscosity, an expression for  $L$  is also required. The length scale,

$L$ , is always mathematically prescribed, in a similar manner to the zero-equation models. Thus, one can now calculate eddy viscosity using equation 2-24.

The transport expression for  $k$  can be derived exactly from the Navier-Stokes equation (Hinze, 1959). The  $k$  equation accounts for convective transport as well as history effects on the characterizing

velocity scale,  $k^{1/2}$ . For high Reynolds number, this equation reads (Rodi, 1980a)

$$\frac{\partial k}{\partial t} + U_i \frac{\partial k}{\partial x_i} = \frac{\partial}{\partial x_i} \left( u_i' \left( \frac{u_j' u_j'}{2} + \frac{p'}{\rho} \right) \right) - u_i' u_j' \frac{\partial U_i}{\partial x_j} + \beta g_i u_i'^3 - \nu \left( \frac{\partial^2 u_i'}{\partial x_j^2} \frac{\partial u_i'}{\partial x_j} - \frac{\partial^3 k}{\partial x_i \partial x_i} \right) \quad (2-25)$$

Since new unknown correlations appear in the above equation, model assumptions must be introduced so the equation can be solved.

These model assumptions are listed in detail in Rodi (1980a).

Introducing these assumptions to terms in the R.H.S of the above equation yields the following

$$\frac{\partial k}{\partial t} + U_i \frac{\partial k}{\partial x_i} = \frac{\partial}{\partial x_i} \left( \frac{\nu_t}{\sigma_k} \frac{\partial k}{\partial x_i} \right) + \nu_t \left( \frac{\partial U_i}{\partial x_j} + \frac{\partial U_j}{\partial x_i} \right) \frac{\partial U_i}{\partial x_j} - \beta g_i \frac{\nu_t}{\sigma_t} \frac{\partial S}{\partial x_i} - C_D \frac{k^2}{L} \quad (2-26)$$

in which

$C_D, \sigma_t, \sigma_k$  = are empirical constants

If Equation 2-26 is applied to an open-channel flow in which the mean velocity  $U$  is parallel to the  $x$  axis and by neglecting convective, diffusive transport as well as the local rate of change, then

production and dissipation terms are in balance. Thus, equation (2-26) is simplified to

$$\nu_t \left( \frac{\partial U}{\partial y} \right)^2 = C_D \frac{k}{L} \quad (2-27)$$

When equation 2-24 is used in equation 2-27 to eliminate  $k$ , a mixing length formula will result.

$$\nu_t = \left( \frac{C_D}{C_D} \right)^{\frac{1}{2}} L^2 \left| \frac{\partial U}{\partial y} \right| \quad (2-28)$$

This demonstrates that the mixing length hypothesis is indeed a special case of one-equation models. In general, the one-equation model is more applicable to a wider range of flow cases than the mixing length hypothesis because these models account for transport and history effects (Rodi, 1980a and 1980b; Reynolds, 1976; Bradshaw, 1972).

One-equation models have offered no improvement with regard to the characteristic length scale. This difficulty resides in the necessity to prescribe the distribution of  $L$ . This is not an easy task to accomplish, especially in a complex flow. Different mixing length scale formulae, however, have been proposed to generally calculate  $L$ , the length scale. These expressions are rather complex and to date have been tested very little (Rodi, 1980a; Reynolds, 1976). In addition, substantial computer time is required to solve the newly proposed formula when compared to more advanced models (Rodi, 1980a). Therefore, the trend has been shifted towards two-equation models in which a transport equation is solved for both the characteristic length scale  $L$ , and the velocity scale  $k^{\frac{1}{2}}$ .

### B-3 Two-equation model

Because mixing length scale is influenced by transport and history effects in the same manner as turbulent velocity, additional equations for the characteristic length scale can be developed. Two-equation models account for both the transport of turbulent velocity and the length scale by solving two transport equations. In contrast to zero and one-equation models, the employment of a transport equation for the mixing length in a two-equation model allows an accurate determination of the length scale distribution even in a complex flow.

Several workers have explored the use of a second turbulence transport equation which, when solved, determines the distribution of  $L$ . For the second transport equation,  $L$  does not have to be the dependent variable. Any representation of  $L$ , for example  $kL$  or  $k/L$ , would yield the desired equation.

Various two-equation models exist e.g.  $k-k_l$ ,  $k-W$ , and  $k-\epsilon$ , (for a complete list see Launder and Spalding, 1974) in which:

- $l$  = a length scale representing the macro-scale of turbulence
- $W$  = a quantity having the dimensions of  $(\text{time})^{-2}$ , which represents the time-average square of vorticity fluctuations, and
- $\epsilon$  = rate of dissipation of turbulent energy.

The various length-scale equations proposed in the literature perform similarly to each other. The  $\epsilon$  equation, developed by Rodi (1980a), has become popular among model developers for several reasons. Workers have concluded that the  $\epsilon$  equation is relatively simple, contains fewer terms than other length scale equations, and  $\epsilon$  appears naturally as an unknown in the turbulent kinetic energy equation (Rodi, 1980a and b; Launder and Spalding, 1974 and 1972). The  $\epsilon$  equation can

also be derived exactly from the Navier-Stokes equations (Reynolds and Cabeci, 1978).

There exist a few transport equations that determine the length scale by themselves or when combined with the k equation i.e. kl, W, and e (for a complete list see Launder and Spalding, 1972). The z equation is selected for this study and reads (Rodi, 1980a)

$$\frac{\partial \epsilon}{\partial t} + U_i \frac{\partial \epsilon}{\partial x_i} = \frac{\partial}{\partial x_i} \left( \frac{\nu_t}{\sigma_\epsilon} \frac{\partial \epsilon}{\partial x_i} \right) + C_{1\epsilon} \frac{\epsilon}{k} (P+G)(1+C_{2\epsilon} R_f) - C_{2\epsilon} \frac{\epsilon^2}{k} \quad (2-29)$$

In which

$C_{1\epsilon}$ ,  $C_{2\epsilon}$ ,  $C_{3\epsilon}$ ,  $\sigma_\epsilon$  = are empirical constants

$$G = -\beta g_i \frac{\nu_t}{\sigma_t} \frac{\partial S}{\partial x_i}, \text{ buoyancy production of } k \quad (2-29a)$$

$$P = \nu_t \left( \frac{\partial U_i}{\partial x_j} + \frac{\partial U_j}{\partial x_i} \right) \frac{\partial U_i}{\partial x_j}, \text{ energy production by shear stress} \quad (2-29b)$$

$$R_f = \text{flux Richardson number} \left( -\frac{G}{P} \right) \quad (2-29c)$$

and the eddy viscosity can be calculated from

$$\nu_t = C_\mu' \frac{k^2}{\epsilon} \quad (2-30)$$

The k-z closure model is equivalent to Mellor and Yamada's (1982) level two and a half model. In this model, closure is obtained by solving an equation for turbulent kinetic energy, k or  $\frac{g}{2}$ , and an equation for qL in which L is the master length scale. All length scales needed for level two and a half model are assumed to be linearly related to the master length scale, L.

Level two and half can also be considered a one-equation model if an empirical formula is employed as the characteristic mixing length scale. Equations that comprise the level two and a half model were first presented and discussed in Mellor and Yamada (1982).

#### B-4 Stress-equation model

One- and two-equation models assume that the local state of turbulence can be characterized by a single velocity scale. Consequently, the individual Reynolds stresses can be related to this scale. This relation often indicates that the transport of the individual stresses is not adequately accounted for, even if the transport of the characterizing velocity has been taken into account (Rodi, 1980a and 1980b). In order to account for the magnitude of individual Reynolds stresses (representing various velocity scales in complex flows), and to properly account for their transport, more elaborate models have been developed. Most of these advanced models employ transport equations for the individual stresses  $\overline{u_i u_j}$ . Analogous transport equations have been introduced for the turbulent mass fluxes  $\overline{u_i s}$ .

Models based on these equations are often referred to as stress-flux-equation models or second-order closure schemes. Stress-flux-equation models are used primarily if the need exists to determine the individual stresses  $\overline{u_i u_j}$ . A second use of these models is to assess lower-level or newly proposed models. Stress-flux-equation models are still under intensive development and are not yet in use for practical or engineering applications.

Based on Rotta's energy redistribution hypothesis as well as local isotropy, Mellor and Yamada (1974) have introduced the level four model. This model consist of solving 13 simultaneous partial differential equations. In addition, they also assumed that all length

scales are linearly related. All constants employed for the length scales were obtained from neutral turbulence data.

The stress-equation models do not use Boussinesq's analogy. Instead, they model the stress terms directly. Exact equations for Reynolds stress can be derived from the Navier-Stokes equations (Tennekes and Lumley, 1972). The stress-equation models are required in flow situations where the knowledge of transport and fluxes are essential and can not be approximated well by relating them to the transport of  $k$ . In free flows, the stress-equation model proposed by Launder, Reece and Rodi (1975), does not appear to perform significantly better than the standard  $k$ - $\epsilon$  model (Rodi, 1980a). The stress-equation models can be used as an approach to improve the simpler one- and two-equation models. This more complex stress-equation model can be used as a guide to the nature of new terms which should be included.

### C. Existing estuary models

Numerous estuarine models exist. Among those of interest are time-dependent multi-dimensional models which calculate vertical eddy viscosity and diffusivity. These models can be classified according to their closure scheme.

#### C-1 Zero-equation model

In this class of models, a constant eddy viscosity or a mixing length formulation is employed for the closure of the governing equations. This empirical constant was found either by trial and error or from observational data. A constant eddy viscosity, employed in most hydraulic applications, resulted in very poor agreement with observations (Dowden and Hamilton, 1975; Wang and Kravitz, 1980).

Kent et al. (1959) and Pritchard (1960), showed that the effects of vertical stability on mixing coefficients can be matched by including an extra factor in the eddy viscosity formulae. This new factor accounts for stratification effect via local Richardson number,  $R_i$ , and the eddy coefficient can be calculated as follows

$$D_i = \frac{D_{t^0}}{(1 + \alpha R_i)^q} \quad (2-31)$$

in which

$$R_i \text{ local Richardson number} = - \frac{g}{\rho} \frac{\left(\frac{\partial \rho}{\partial z}\right)}{\left(\frac{\partial U}{\partial z}\right)^2} \quad (2-32)$$

$\alpha, q$  = are empirical constants, and

$D_{t^0}$  = eddy coefficient under neutral stability.

Pritchard's empirical formula is divided into two parts. The first part accounts for a mean-flow-induced turbulence and the second part accounts for the wind-induced turbulence at the surface. This formula was developed to fit the observational results for mass exchange coefficient in the James River Estuary and was utilized later by other workers for their mixing length models (e.g. Kuo et al., 1978).

Bowden and Hamilton (1976) have reviewed three different methods that describe the eddy viscosity: 1- Eddy viscosity taken as a constant 2- Eddy viscosity was taken as a function of water depth and mean current, i.e. a function of time and 3- Eddy viscosity was taken as a function of Richardson number.

They added an extra term into their eddy viscosity formulation. This extra term assures a value for the eddy viscosity when a velocity reversal occurs (at times near slack water). They reason that when the velocity goes to zero, a residual turbulence should be present.

Bowden and Hamilton (1976) conclude that best agreement is obtained by taking eddy viscosity as a function of the instantaneous Richardson number (function of time). They also reported that the actual function they used was not valid over the entire range of conditions. In addition, they stated that if a better agreement between prediction and observation is to be achieved, knowledge of the functional form and magnitude of these parameters that correspond to real conditions is necessary.

Elliott(1976) arrived at a conclusion that realistic stratification can not be obtained with a constant eddy viscosity. Therefore, Elliott used a varying eddy viscosity incorporating a bulk Richardson number and time-depth dependency. Although his formulation produced a more realistic salinity distribution than that obtained by Bowden and Hamilton, he concluded that this method still required further careful examination. With regard to horizontal diffusivity, Elliott (1976) suggests that it bears little or no effect on the solution, implying that the vertical eddy viscosity is predominant in estuaries.

Blumberg (1977) used a stability dependent eddy viscosity in an application to the Potomac River estuary. His study demonstrated that salt intrusion is very sensitive to the eddy viscosity.

In their study of the turbidity maximum in the Rappahannock Estuary, Kuo et al. (1978) concluded that suspended sediment, or mass distribution, is highly sensitive to the vertical eddy viscosity. They employed the same stability dependent formula proposed by Pritchard (1960) and concluded that the model can be used only for qualitative interpretation.

Applying his model to the James River estuary, Cerco (1982), addressed the problem of accurately computing the eddy viscosity terms. He reported that the functional form should consider four related aspects: 1- The expression should account for the magnitude of turbulent diffusion in a homogeneous flow 2- The expression should incorporate a stratification parameter 3- The expression should appropriately relate diffusivity and diffusion of momentum and 4- The functional form should be time dependent if a proper simulation for the mean parameters is to be achieved. His approach was to employ a form, suggested by Officer (cited from Cerco, 1982), in which stratification effects on the vertical eddy viscosity can be accounted for by the Richardson number. In order to consider the diffusion in a homogeneous flow, he used the following linear expression

$$K_z = \frac{K_0}{(b + \alpha R_1)^n} \quad (2-33)$$

$$K_0 = a U \quad (2-34)$$

in which

$K_0$  = eddy diffusion in a well mixed water column, and  
 $a, b, n, \alpha$  = empirical constants.

Evaluation of the above constants was made through a series of model runs which resulted in a tidal-average eddy diffusivity which falls in the range reported by Harleman and Ippen (1967).

In summary, when compared with observations, the use of constant eddy coefficients result in a poor and unrealistic model simulation. The results are improved by using semi-empirical formulations. Better agreement is obtained through expressions which account for stratification via  $R_1$ . The improved results are limited to specific

applications. Models employing the mixing-length hypothesis as a closure scheme for the governing equations require empirical input in the form of constants. These constants must be determined, or tuned in, for each flow case. The need to adjust these constants for each application limit the use of this class of models. Although semi-empirical formulation resulted in a good agreement with observations, investigators urged other workers to further examine these formulations (Bowden and Hamilton, 1976 ; Elliott, 1976).

#### C-2 Advanced-closure models

Smith and Takhar (1981) applied a one-equation model to an idealized straight rectangular channel, similar in dimensions to the Rotterdam waterway. In this model the eddy viscosity was determined by solving the turbulence energy equation and an expression for  $L$ , which they previously derived (Smith and Takhar, 1979). They demonstrated that the representation of Reynolds fluxes in estuaries employing this closure scheme overcame the need to add an extra term to the eddy viscosity formulae in order to account for turbulence during slack water.

As mentioned earlier in this chapter, Mellor and Yamada (1982) added a new level of turbulence closure models to their classification. This new model, labeled level two and a half, is a simplified version of their level three model. This version is equivalent to the  $k-\epsilon$  model. The velocity scale equations are not quite similar referring to the way buoyancy terms are modeled. The  $k-\epsilon$  model employs the exact buoyancy term, while the level two and a half model determines these via stability function. As for mixing length, the main difference between

these two length scale equations are the constants employed in each equation. It has been demonstrated by various workers that constants employed in the k- $\epsilon$  model do not require adjustment to each individual application. All model applications were made through the standard constants cited from literature. On the other hand, two of the constants employed in the length scale equation by Mellor and Yamada (1982) have to be adjusted for each case. They also stated that "One can not assert great confidence in equation (48). We prefer it rather than the differential equation for dissipation used by Daly and Harlow ...". Equation 48, that they refer to, is the mixing length formula employed in their closure scheme. The same equation that was used by Daly and Harlow (1970) is equation 2-29 in this investigation. As stated earlier, all mixing length equations perform similarly to each other. Therefore, one should investigate the overall model results rather than how the individual mixing length equation behaves. For the level two and a half an empirical formula for the length scale can also be employed instead of solving a complete transport equation for the characteristic mixing length scale. If such an approach is taken, then the level two and a half is classified as a one-equation model.

Oey, Mellor and Hires (1985) employed a level two and a half turbulent closure scheme in their application of the three-dimensional time-dependent model to the Hudson-Raritan estuary. They reported that results from current simulations compared reasonably well with field observations except at narrow channel regions where the model resolution is inadequate.

Celik and Rodi (1985) applied the k- $\epsilon$  model to a small portion of the Humber estuary in order to calculate the variation of the eddy

viscosity in the vertical plane at various time intervals. Model predictions of the eddy coefficients have been shown to be in good agreement with observations made by other workers. A drastic temporal and spatial change of the predicted and observed eddy viscosity was noted. From such results Celik and Rodi (1985) concluded that a constant or a simple function of the vertical distance can not approximate the eddy viscosity.

The empirical constants employed in their k- $\epsilon$  model were given the standard values cited in literature. These constants were not adjusted to fit the experiments or observation. They also reported that temporal and spatial variations of the velocity field can be predicted satisfactorily in wave-induced turbulent flow by the k- $\epsilon$  model.

It should be noted that the Humber estuary is well-mixed with nearly uniform vertical salinity distribution. Therefore, buoyancy effects can be (and were) neglected in their study. Most estuaries however, have nonuniform salinity distributions which result in considerable stratification and require a proper presentation of buoyancy terms in the k- $\epsilon$  model.

Rastogi and Rodi (1978) compared a two- versus a three-dimensional model in which closure of the governing equations was accomplished by an advanced turbulence model. The k- $\epsilon$  closure introduced for the two-dimensional depth integrated model does not account for the influence of buoyancy. Nevertheless, at high Froude numbers, comparisons of the 2-D and 3-D model predictions show good agreement for different velocity ratios and river bed roughness. The same well established standard empirical constants, cited in literature,

were employed again for this comparison which demonstrated the generality of the  $k-\epsilon$  model.

Models employing transport equations for individual turbulent stresses and fluxes predict the turbulent processes more realistically than simpler models. On the other hand, they have been tested very little and computationally are more expensive than one- and two-equation models.

Concerning the choice of a suitable turbulence model, it seems that the level two model is most promising in terms of its extent of applicability and simplicity. For this study, the level two model is chosen as a representative of Mellor's and Yamada's (1974, 1980) classification. Furthermore, the  $k-\epsilon$  model is selected to represent the other school of thought (Rodi, 1980a). The  $k-\epsilon$  model requires the solution of two additional partial differential equations, which will substantially increase computational time for most applications. On the other hand, the level two model does not require the solution of extra equations. Instead, an algebraic expression for the stability function is needed. Hence, lengthy computational time is not a major characteristic of the level two models. It has been suggested that the level two model and  $k-\epsilon$  model have a very wide range of applicability and are superior to models that employ the mixing length hypothesis. According to the preceding literature review, the choice of the  $k-\epsilon$  and level two model is favoured. Each of these models presents a different school of thought and thus pose an interesting challenge to see how they perform individually and in comparison to one another. These two models have been selected as the closure scheme for the equations governing the mean flow variables for the undergoing investigation. This set of

equations describing the dynamics of an estuary, are derived in the following chapter. The equations are then put in a numerical scheme to be solved by a computer.

## CHAPTER III.

### FINITE DIFFERENCE FORM FOR THE k- $\epsilon$ MODEL

This chapter is subdivided into three major sections. The first, A, shows how the two closure schemes are incorporated with the governing equations. The second, B, deals with the derivation of the turbulent closure scheme. The k and  $\epsilon$  equations are integrated laterally in section B-1 and vertically in section B-2. Production terms that appear in k and  $\epsilon$  equations will be shown as "SRC" throughout this chapter. Since these terms require special treatment, they will be integrated separately in chapter 4. The third and final section, C, is devoted to the finite difference formulation. The final form of k and  $\epsilon$  equations are then expressed in the finite difference form.

The present study adopts a right-hand coordinate system in which the origin is located at the undisturbed free surface at the head of the estuary. The x axis is positive, directed towards the mouth of the estuary. The y axis is positive to the right, facing upstream, while the z axis is positive upward as shown in figure 3.1.

#### A. Governing equations:

The basic set of equations that represent and determine the flow field and salinity structure of an estuary, in space and time, are the momentum balance equation, the salt conservation equation, the continuity equation and an equation of state. Application of Reynolds

rule of averaging, and by noting the assumptions stated earlier in Chapter 2, results in the following set of equations

$$\frac{\partial U_i}{\partial t} + U_j \frac{\partial U_i}{\partial x_j} = - \frac{1}{\rho_0} \frac{\partial P}{\partial x_i} - \frac{\partial}{\partial x_j} (\overline{u_i' u_j'}) + \epsilon_i \left( \frac{\Delta \rho}{\rho_0} \right) \quad (3-1)$$

$$\frac{\partial U_i}{\partial x_i} = 0 \quad (3-2)$$

$$\frac{\partial S}{\partial t} + \frac{\partial}{\partial x_i} (U_i S) = - \frac{\partial}{\partial x_i} (\overline{u_i' s'}) \quad (3-3)$$

$$\rho = \rho_0 (1.0 + \beta S) \quad (3-4)$$

Simplification of the governing equations can be obtained by applying the boundary-layer approximation. This approximation states that the velocity shear  $\frac{\partial U}{\partial x_3}$  is predominant, which implies that only vertical turbulent diffusion is significant. Thus, the proposed model in its final form can be written as:

$$\frac{\partial U_i}{\partial t} + U_j \frac{\partial U_i}{\partial x_j} = - \frac{1}{\rho_0} \frac{\partial P}{\partial x_i} - \delta_{i3} \frac{\partial}{\partial x_3} (\overline{u_i' u_3'}) + \epsilon_i \delta_{i3} \left( \frac{\Delta \rho}{\rho_0} \right) \quad (3-5)$$

$$\frac{\partial U_i}{\partial x_i} = 0 \quad (3-6)$$

$$\frac{\partial S}{\partial t} + \frac{\partial}{\partial x_i} (U_i S) = - \frac{\partial}{\partial x_3} (\overline{u_3' s'}) \quad (3-7)$$

$$\rho = \rho_0 (1.0 + \beta S) \quad (3-8)$$

for the k- $\epsilon$  model Reynolds stress can be modeled as follows:

$$-\overline{u_i' u_j'} = \nu_t \frac{\partial U_i}{\partial x_j}, \quad \text{if } i = 1, j = 3 \text{ and } = 0, \text{ otherwise} \quad (3-9)$$

where

$$\nu_t = c_\mu \frac{k^2}{\epsilon} \quad (3-9a)$$

and for level two model Reynolds stress can be replaced by:

$$-\overline{u_i u_j} = L^2 S_m \left( \frac{\partial U}{\partial x_i} \right)^2, \text{ if } i = 1, j = 3 \text{ and } = 0, \text{ otherwise} \quad (3-10)$$

Reynolds flux can be approximated by the k- $\epsilon$  model as follows:

$$-\overline{u_i s} = \frac{U}{\sigma_t} \frac{\partial S}{\partial x_i}, \text{ if } i = 3 \text{ and } = 0, \text{ otherwise} \quad (3-11)$$

and by the level two model as follows:

$$-\overline{u_i s} = L^2 S_h \left( \frac{\partial U}{\partial x_i} \right) \left( \frac{\partial S}{\partial x_i} \right), \text{ if } i = 3 \text{ and } = 0, \text{ otherwise} \quad (3-12)$$

in which

$S_m$  and  $S_h$  are the stability functions defined in Chapter 2.

Since parameter variations across estuaries are usually small compared to longitudinal variations, the above equations can be further simplified by lateral integration. Cerco (1982) has integrated the equations governing the mean flow. He also described how these equations can be expressed in finite difference form. These procedures will not be repeated here. Instead, the proposed closure schemes will be integrated laterally, vertically and then expressed in finite difference form. It should be noted that it is the k and  $\epsilon$  equations that need to be integrated whereas the level two model is an algebraic expression which can be solved easily by a computer and need not be integrated.

#### A-1 Turbulence closure scheme (k- $\epsilon$ ).

The simplified set of equations 3-5 through 3-8 are not closed for reasons stated earlier. The system of equations can be solved if and only if Reynolds stresses  $u_i u_j$  and turbulent fluxes  $u_i s$  can be only if Reynolds stresses  $u_i u_j$  and turbulent fluxes  $u_i s$  can be

determined. A two-equation turbulence closure model (k-ε) is employed as one part of this study. The two partial differential equations, which together comprise the k-ε model in full for high Reynolds number, are previously stated in Chapter 2 (equations 2-26 through 2-29). The standard k-ε model is based on the assumption that eddy viscosity is the same for all Reynolds stresses  $\overline{u_i u_j}$  (isotropic eddy viscosity). The calculation of  $\overline{u_i u_j}$  in estuaries is not influenced by this assumption because only the shear stress  $\overline{u w}$  is important in these flows (Rodi, 1980a). In addition, Rodi (1980a,b) reported that the constant  $C_{3\epsilon}$  is approximately equal to zero for vertically buoyant shear flow. Thus, the proposed k-ε model in its final form reads

$$\frac{\partial k}{\partial t} + U_i \frac{\partial k}{\partial x_i} = \frac{\partial}{\partial x_i} \left( \frac{V_t}{\sigma_k} \frac{\partial k}{\partial x_i} \right) + P + G - \epsilon \quad (3-12)$$

$$\frac{\partial \epsilon}{\partial t} + U_i \frac{\partial \epsilon}{\partial x_i} = \frac{\partial}{\partial x_i} \left( \frac{V_t}{\sigma_\epsilon} \frac{\partial \epsilon}{\partial x_i} \right) + C_{1\epsilon} \frac{\epsilon}{k} (P+G) - C_{2\epsilon} \frac{\epsilon^2}{k} \quad (3-13)$$

All parameters in these equations have been defined in Chapter 2.

If boundary layer approximations are introduced to equations (3-12) and (3-13), one can write:

$$\begin{aligned} \frac{\partial k}{\partial t} + U \frac{\partial k}{\partial x} + w \frac{\partial k}{\partial z} &= \frac{\partial}{\partial x} \Gamma_x \frac{\partial k}{\partial x} + \frac{\partial}{\partial z} \left( \frac{V_t}{\sigma_k} \frac{\partial k}{\partial z} \right) \\ &+ P - G - \epsilon \end{aligned} \quad (3-14)$$

$$\begin{aligned} \frac{\partial \epsilon}{\partial t} + U \frac{\partial \epsilon}{\partial x} + w \frac{\partial \epsilon}{\partial z} &= \frac{\partial}{\partial x} \Gamma_x \frac{\partial \epsilon}{\partial x} + \frac{\partial}{\partial z} \left( \frac{V_t}{\sigma_\epsilon} \frac{\partial \epsilon}{\partial z} \right) \\ &+ C_{1\epsilon} \frac{\epsilon}{k} (P+G) - C_{2\epsilon} \frac{\epsilon^2}{k} \end{aligned} \quad (3-15)$$

in which

$\Gamma_x$  = longitudinal dispersion due to transverse velocity shear

The production term, P in equations (3-12) and (3-13), will be evaluated in more detail in Chapter 4. Therefore, P will be excluded from integration in the following sections.

### B-1 Lateral integration

Further reduction is accomplished if the k and ε equations are integrated along the y axis. This simplification is obtained by assuming that all variables are independent of y and by employing Liebnitz' rule. The laterally integrated k and ε equations are:

$$\begin{aligned} \frac{\partial}{\partial t} Bk + \frac{\partial}{\partial x} BUk + \frac{\partial}{\partial z} BWk = & \frac{\partial}{\partial x} \left( \int_x B \frac{\partial k}{\partial x} \right) + \frac{\partial}{\partial z} \left( \frac{V_t}{\sigma_k} B \frac{\partial k}{\partial z} \right) \\ & + SRC + \beta_k \left( \frac{V_t}{\sigma_t} B \frac{\partial S}{\partial z} \right) - \epsilon B \end{aligned} \quad (3-16)$$

$$\begin{aligned} \frac{\partial}{\partial t} B\epsilon + \frac{\partial}{\partial x} BU\epsilon + \frac{\partial}{\partial z} BW\epsilon = & \left( \frac{\partial}{\partial x} \left( \int_x B \frac{\partial \epsilon}{\partial x} \right) + \frac{\partial}{\partial z} \left( \frac{V_t}{\sigma_\epsilon} B \frac{\partial \epsilon}{\partial z} \right) - C_{2\epsilon} \frac{\epsilon^2}{k} B \right) \\ & + SRC + C_{1\epsilon} \frac{\epsilon}{k} \left( \beta_\epsilon \frac{V_t}{\sigma_t} B \frac{\partial S}{\partial z} \right) \end{aligned} \quad (3-17)$$

### B-1-2 Vertical integration

As mentioned earlier, grid spacing in the vertical direction will result in a number of horizontal slices to which the k and ε equations are also applicable. Vertical integration is accomplished by assuming all variables are constant over the depth of each layer. Employing the mean value theorem for integrals to buoyancy terms in both the k and ε equations along with Liebnitz' rule yields:

$$\frac{\partial}{\partial t} Bkh + \frac{\partial}{\partial x} BUkh + (BWk)_T - (BWk)_b = \frac{\partial}{\partial x} \left( \int_x hB \frac{\partial k}{\partial x} \right) + SRC + \left( \frac{V_t}{\sigma_k} B \frac{\partial k}{\partial z} \right)_T - \left( \frac{V_t}{\sigma_k} B \frac{\partial k}{\partial z} \right)_b$$

$$- zBh + \beta E_s \left( \frac{V_t}{\sigma_t} B \right) (S_T - S_b) \quad (3-19)$$

$$\begin{aligned} \frac{\partial}{\partial t} B \epsilon h + \frac{\partial}{\partial x} B U \epsilon h + (B W z)_T - (B W z)_b &= \frac{\partial}{\partial x} \left( \int_x h B \frac{\partial \epsilon}{\partial x} \right) + SRC + C_{1z} \frac{z}{k} B h \\ &+ \left( \frac{V_t}{\sigma_t} B \frac{\partial \epsilon}{\partial z} \right)_T - \left( \frac{V_t}{\sigma_t} B \frac{\partial \epsilon}{\partial z} \right)_b \\ &+ \frac{z}{k} C_{1z} \beta E_s \left( \frac{V_t}{\sigma_t} B h \right) (S_T - S_b) \end{aligned} \quad (3-20)$$

in which

$h$  = layer thickness

T,b= subscripts denoting parameter evaluated at top and bottom of a layer respectively

### C. Finite Difference Formulation

An analytical solution for the complete set of equations does not exist. In order to solve this system of equations, a numerical approach is taken. In the finite difference formulation, all continuous variables are replaced by discrete variables on a uniform staggered grid. The grid used for this study is shown in figure 3.1. Application of the boundary conditions was made easier by using a staggered grid as will be shown later.

The channel was subdivided into subvolumes in which the longitudinal index,  $i$ , increased from the head,  $i=1$ , to the mouth of the channel,  $i=L$ . The vertical index,  $k$ , increased from the surface,  $k=1$ , to the bottom layer,  $k=n$ . Distance between longitudinal nodes is denoted by  $\Delta x$ , and vertical distance between layers is set equal to  $\Delta z$ . To indicate the time step, a superscript ' is used for future time step ( $n+1$ ). No superscript represents present time step ( $n$ ). It should be

also noted that the estuary width,  $B$ , is a function of only  $x$  and  $z$ . The surface level elevation,  $\eta$ , is a function of  $x$  and  $t$ , and the layer thickness,  $h$ , is only a function of  $t$  for the surface layer and a function of  $x$  for the remaining layers.

The representation of variables used in numerical integration can vary widely. The elected scheme, however, should provide a stable and convergent solution to the original partial differential equations. A semi-implicit scheme was developed by Cerco (1982) and has been proven to meet such requirements. The finite difference technique adopted for this study is the same as the one employed by Cerco (1982). Full details of the numerical solution for equations governing the mean flow are described in details elsewhere (Cerco, 1982). Therefore, attention will only be given to the equations that comprise the turbulent closure scheme.

### C-1 Formulation of the energy equation

In the finite difference formulation, the grid points where  $U$  and  $\Gamma$  are evaluated are those points at which vertical and horizontal velocities are calculated, respectively.

The integrated discretized form of the  $k$ -equation (3-19) for the surface layer is:

$$\begin{aligned} & \left[ \frac{B_{i,k} k'_{i,k} (\Delta z + \eta'_i) - B_{i,k} k_{i,k} (\Delta z + \eta_i)}{\Delta t} \right] + \left[ \frac{T5_{i,k} - T5_{i-1,k}}{\Delta x} \right] - WkB \\ & = - \text{DIFB} (k_{i,k} - k'_{i,k+1}) + \left[ \frac{T6_{i,k} - T6_{i-1,k}}{\Delta x} \right] \\ & \quad + \text{SRC} + \varepsilon B (\Delta z + \eta_i) \end{aligned} \quad (3-21)$$

in which

$$\begin{aligned}
T5_{i,k} &= U_{i+1,k} \bar{B}_{i,k} (\Delta z + \bar{\eta}'_i) [(k_{i,k} + k_{i+1,k}) / 2.] \\
T6_{i,k} &= \int_x \bar{B}_{i+1,k} (\Delta z + \bar{\eta}'_{i+1}) (k_{i+1,k} - k_{i,k}) \\
\bar{B}_{i,k} &= (B_{i,k} + B_{i+1,k}) / 2. \\
WkD &= W_{i,k} [(B_{i,k} + B_{i,k+1}) / 2.] [(k_{i,k} + k_{i,k+1}) / 2.] \\
DIFB &= \frac{V_t}{\sigma_k} \left( \frac{B_{i,k} + B_{i,k+1}}{2} \right) \left( \frac{k'_{i,k} + k'_{i,k+1}}{2} \right)
\end{aligned}$$

A similar equation for the remaining subsurface layers can be written if  $\eta_i$  in equation (3-21), is set equal to zero and by adding the appropriate terms to account for vertical transport and diffusion through the surface of each layer. Thus, the generalized form of the energy equation, applicable to subsurface layers is:

$$\begin{aligned}
-k'_{i,k-1} ADA2 + DIFT + k'_{i,k} [1 + ADA2 (DIFT + DIFB)] \\
-k'_{i,k+1} ADA2 + DIFB = k_{i,k} - ADA2 \left\{ \frac{T5_{i,k} - T5_{i-1,k}}{\Delta x} \right\} \\
- ADA2 [WkT - WkB] \\
+ ADA2 [SRC + B_{i,k} \Delta z \epsilon] \quad (3-22)
\end{aligned}$$

in which

$$\begin{aligned}
WkT &= W_{i,k-1} [(B_{i,k} + B_{i,k-1}) / 2.] [(k_{i,k} + k_{i,k-1}) / 2.] \\
DIFB &= \frac{V_t}{\sigma_k} \left( \frac{B_{i,k} + B_{i,k-1}}{2} \right) \left( \frac{k'_{i,k} + k'_{i,k-1}}{2} \right)
\end{aligned}$$

Equation (3-21) is in a tridiagonal form which can be solved by matrix methods if vertical boundary conditions are provided. As mentioned earlier, there is no energy flux through solid boundaries or at the free surface. The boundary condition employed herein is as follows

$$V_t \frac{\partial k}{\partial z} = 0 \quad z = \eta \quad (3-23a)$$

$$V_t \frac{\partial k}{\partial z} = 0 \quad z = -\Pi \quad (3-23b)$$

### C-2 Formulation of the energy dissipation equation

The  $z$  equation (3-20) remains to be expressed in a discrete form for surface and subsurface layers. The  $z$  equation is treated in a similar manner to the  $k$  equation. The discrete form of the energy dissipation equation, applicable to the surface layer, is presented below

$$\begin{aligned} & \left[ \frac{B_{i,k} \epsilon'_{i,k} (\Delta z + \eta'_i) - B_{i,k} \epsilon'_{i,k} (\Delta z + \eta'_i)}{\Delta t} \right] + \left[ \frac{T7_{i,k} - T7_{i-1,k}}{\Delta x} \right] - WzB \\ & = - \text{DIFB} ( \epsilon'_{i,k} - \epsilon'_{i,k+1} ) + \left[ \frac{T8_{i,k} - T8_{i-1,k}}{\Delta x} \right] \\ & + \text{SRC} + C_{ze} \frac{g}{k} B_{i,k} (\Delta z + \eta'_i) \end{aligned} \quad (3-25)$$

in which

$$\begin{aligned} T7_{i,k} &= U_{i+1,k} \bar{B}_{i,k} (\Delta z + \bar{\eta}'_i) [(z_{i,k} + z_{i+1,k}) / 2.] \\ \text{DIFB} &= \frac{U_{t,i,k}}{\sigma_e} \left( \frac{B_{i,k} + B_{i,k+1}}{2} \right) \left( \frac{\epsilon'_{i,k} + \epsilon'_{i,k+1}}{2} \right) \end{aligned}$$

For subsurface layers the final equation is

$$\begin{aligned} -\epsilon'_{i,k+1} \text{ADA2} + \text{DIFT} + \epsilon'_{i,k} [ 1 + \text{ADA2} (\text{DIFT} + \text{DIFB}) ] = \\ + \epsilon'_{i,k} - \text{ADA2} \left[ \frac{T7_{i,k} - T7_{i-1,k}}{\Delta x} \right] - \text{ADA2} [ WzT - WzD ] \\ + \text{ADA2} \left[ \text{SRC} + C_{ze} B_{i,k} \Delta z \frac{g}{k_{i,k}} \right] \end{aligned} \quad (3-26)$$

where

$$\begin{aligned} WzT &= W_{i,k-1} ( B_{i,k} + B_{i,k-1} ) / 2 \cdot ( \epsilon'_{i,k} + \epsilon'_{i,k-1} ) / 2. \\ \text{DIFT} &= \frac{U_{t,i,k-1}}{\sigma_e} \left( \frac{B_{i,k} + B_{i,k-1}}{2} \right) \left( \frac{\epsilon'_{i,k} + \epsilon'_{i,k-1}}{2} \right) \end{aligned}$$

Equation (3-26) is in a tridiagonal form which can be solved by matrix methods providing the appropriate vertical boundary conditions at the free surface and at the river bed are imposed. The boundary conditions employed are

$$\mathcal{V}_t \frac{\partial z}{\partial z} = 0 \quad \text{at } z = \eta \quad (3-27a)$$

$$\mathcal{V}_t \frac{\partial z}{\partial z} = 0 \quad \text{at } z = -\Pi \quad (3-27b)$$

### C-3 Boundary condition for k and e equations

In an ideal case, profiles of k and e measured along the boundaries of the calculation domain are desired. This information, however, is not always available. Therefore, one must construct an appropriate, yet consistent, boundary condition for k and e equations.

At the open end of an estuary, a common practice is to extrapolate for horizontal velocities to a fictitious transect outside the estuary. The same technique is applied for k and e at the open end

$$\frac{\partial^2 k}{\partial x^2} = \frac{\partial^2 e}{\partial x^2} = 0 \quad \text{at } x = L$$

At the upstream end a different approach is taken. The initial and boundary conditions at the most upstream transect are dependent upon the inflow conditions. Eddy viscosity is calculated from

$$\mathcal{V}_t = 0.0765 U_* h \quad (3-29)$$

$$e = S_o g U \quad (3-30)$$

$$\mathcal{V}_t = C \frac{k^2}{\nu} \quad (3-31)$$

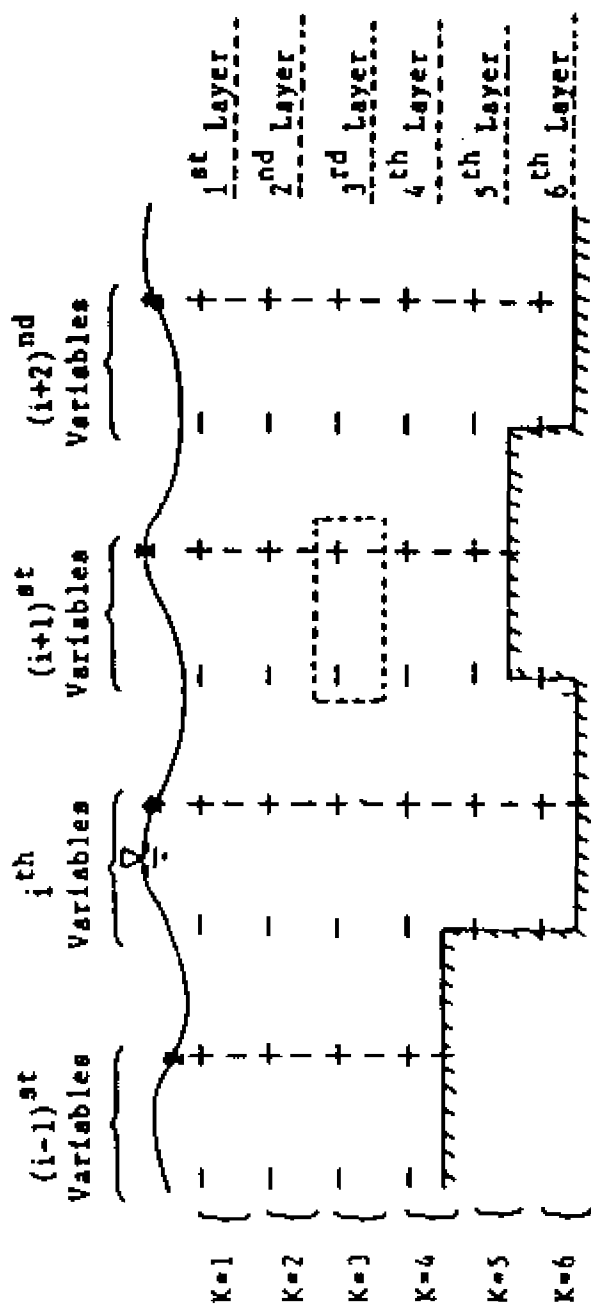
in which

$S_o$  = surface slope

$U_*$  = friction velocity

In a case where the fresh water input at the upstream end is zero, a different method is adopted. Uniform values of k and e are selected in a manner such that the resultant eddy viscosity is very large when compared with molecular viscosity ( $\sim 100 \mathcal{V}_o$ ).

Figure 3.1 : Finite difference grid and axis orientation



## CHAPTER IV.

### VERIFICATIONS AND APPLICATIONS

#### OF THE $k-\epsilon$ MODEL

In order to assure that the governing equations along with the closure model have been formulated correctly, several computational tests were conducted. The purpose of these tests is to assure that approximation used in integrating different terms in the governing equations are valid. Section A is devoted to derivation and selection of approximations for the production terms that appear in the  $k$  and  $\epsilon$  equations. The applicability of the model to a nonbuoyant open channel flow is presented and discussed in section B. The final subsection, C, is devoted to the application of the standard  $k-\epsilon$  model in a continuously stratified open channel flow in which stratification can have a pronounced effect on circulation.

It should be noted that, unless stated otherwise, all test runs are made with a uniform rectangular cross-section channel.

#### A. Treatment of energy production terms

In this section special attention will be given to the energy production terms which appears in equation 3-14 and 3-15. Since there exist no analytical solution to integrate these terms, two different approaches have been suggested as an approximation for these terms.

Derivation and boundary conditions employed for the two methods will be presented first. The results obtained for each case, by the two different methods, will be noted. These results are then compared with analytical solutions, if possible, and with each other. A preference is then made towards a single approach based on the results obtained. A naming convention is chosen to refer to each approach. The first approach will be referred to as method A while the second is referred to as method B.

#### A-1 Method A

The energy production term,  $P$ , can be attributed to two different mechanisms. First, production of energy due to velocity shear along the interface between fluid layers,  $P_1$ . Second, production of energy due to the flow interaction with the solid boundary at the river bed,  $P_2$ .

Therefore, the production term  $P$ , in equation (3-14), can be written as

$$P = P_1 + P_2 \quad (4-1)$$

Rastogi and Rodi (1978) and Rodi (1980a) reported that  $P_2 \gg P_1$  due to the presence of a solid boundary at the bottom. An order of magnitude analysis shows that the first term in equation (4-1) can be neglected for all fluid layers since velocity shear between fluid layers is small. An expression for  $P_2$ , applicable to the bottom layer, is derived in the following section.

In a two-dimensional uniform open channel flow, the bottom shear stress can be defined as follows (Henderson, 1966, Fischer et. al., 1976)

$$\frac{\tau}{\rho} = U_*^2 = c_1 U^2 = \nu_t \left( \frac{\partial U}{\partial z} \right) \quad (4-2)$$

in which

$\tau$  = bottom shear stress

$U_*$  = friction velocity

$z$  = is positive vertically upward

$c_1$  = an empirical constant

From equation (2-29b), energy production for a uniform open channel flow is defined as

$$P_1 = \mathcal{V} \left( \frac{\partial U}{\partial z} \right)^2 \quad (4-3)$$

substituting equation (4-2) into (4-3) results in:

$$P_1 = c_1 U^3 \frac{\partial U}{\partial z} \approx c_1 U^3 \frac{U}{H} \quad (4-4)$$

From equation (4-2) friction velocity can be related to the local velocity as follows

$$U = \frac{1}{(c_1)^{1/3}} U_* \quad (4-5)$$

The constant appearing in equations (4-4) and (4-5) will be determined later in this section. Substituting for  $U$ , as defined in (4-5), into equation (4-4), the energy production term  $P_1$  becomes

$$P_1 = P = C_k \frac{U_*^3}{H} \quad (4-6)$$

in which

$H$  = total depth

$$C_k = \frac{1}{c_1}$$

Since  $\epsilon$  is the rate at which  $k$  is being dissipated, it can be written as

$$\epsilon \approx \frac{P_1}{T}$$

where

$T$  = is the time scale of energy dissipation approximated by

$$T \approx \frac{H}{U} \quad (4-7)$$

Therefore, the production term,  $P$ , in the  $\epsilon$  equation becomes

$$C_{12} \frac{g}{k} P = C_e \frac{U_*^4}{H^3} \quad (4-8)$$

in which

$C_e$  = an empirical constant, also to be determined in the following section.

Assuming that a state of local equilibrium exists near the wall region, for homogeneous flow equations (3-14) and (3-15) reduce to

$$C_k \frac{U_*^3}{H} - \epsilon = 0. \quad (4-9)$$

$$C_e \frac{U_*^4}{H^3} - C_2 \frac{g}{k} P = 0. \quad (4-10)$$

Furthermore,  $\epsilon$ , the rate of energy dissipation, and  $U_*$ , the friction velocity, are related to energy slope,  $S_o$ , via

$$\epsilon = S_o g U \quad (4-11)$$

$$U_* = (S_o g H)^{1/2} \quad (4-12)$$

Substituting equation (4-11) and (4-12) into (4-9) and (4-10) it can be shown that

$$C_k = 1 / (C_f)^{1/2} \quad (4-13)$$

and

$$C_e = 3.6 \frac{C_2 C_f^{1/2}}{(C_f)^{1/2}} \quad (4-14)$$

$$C_f = \frac{g n^2}{H^{1/3}} \quad (4-14a)$$

where

$n$  = Manning's coefficient

which are the values needed to evaluate energy production terms in equations (4-6) and (4-8).

## A-2 Method B

In this approach production terms are integrated numerically in all but the last layer near the channel bed. As for the bottom layer, very near the wall, a constant boundary condition is employed for both the energy equation and its dissipation rate. In the absence of buoyancy forces and where conditions for local equilibrium prevail, shear production is in balance with viscous dissipation. This, together with the universal law of the wall will result in the following boundary conditions (Rodi, 1985)

$$k = U_*^3 / C_\mu^3 \quad (4-15)$$

$$\epsilon = U_*^3 / k'y \quad (4-16)$$

in which

$C_\mu$  = constant

$k'$  = Von Karman constant ( taken as 0.40 )

$y$  = distance from solid boundary

At this point it is important to emphasize that both approaches are only an approximation to an exact term. In order to assure that these approximations and model assumptions introduced to various terms in the original equations are valid, one should compare results obtained by the numerical scheme selected with a known analytical solution. In all the following tests a channel of constant rectangular cross-sectional, with a large width to depth ratio, is used unless stated otherwise. In all test runs, time and distance steps,  $\Delta t$  and  $\Delta x$ , are fixed at 207 seconds and 4000 meters respectively. Layer thickness,  $\Delta z$ , is chosen to be 2 meters. Results obtained by methods A and B are presented in the following section.

## B. Model verifications in steady nonbuoyant channel flow

Knight and Ridgeway (1976) have discussed the analytical solutions in a frictionless homogeneous open channel flow when tidal forces are included. They showed that there exists a phase lag between surface and bottom velocities when frictional forces are present. They also showed that by decreasing frictional forces the analytical solution leads to a symmetric tidal wave (e.g. phase lag is zero). Results obtained by method A are presented in figure 4.1 while figure 4.2 presents results obtained by method B. It should be noted that a small Manning's coefficient (0.0001) is employed to simulate the frictionless case runs. From these plots it is quite evident that there is no phase lag between top and bottom velocities which is in agreement with the analytical solution. In addition, one may conclude that the two approaches employed herein are reasonable and valid approximations.

If significant frictional forces are introduced to such a channel, the analytical solution leads to a non-zero phase difference between surface and bottom velocities. Model results, obtained by methods A and B, for open channel flow with friction and tide included are shown in figure 4.3 and 4.4. In these figures the x axis presents time for one tidal cycle and the y axis presents depth of channel. Vertical lines in figure 4.3 and 4.4 are lines of equal velocities (isotachs). From these figures it is clear that bottom velocity reaches slack before flood or ebb before surface velocity (isotach = 0.0) when employing method A. Figure 4.4, method B, does not show a similar feature. Knight and Ridgeway (1976) have shown that the analytical solution leads to a non-zero phase lag between surface and bottom velocities and verified their conclusion in various laboratory experiments.

Assuming a constant eddy viscosity with tidal forces included, it is possible to obtain an analytical solution for velocity as a function of depth. Since the analytical solution is based on a constant eddy viscosity while model results are obtained by calculating eddy viscosity, they cannot be compared. On the other hand, the velocity overshoot at some distances from the boundary, obtained by the analytical solution, has been verified experimentally (Nielsen, 1985). If the model also shows such a feature then evidence suggests that the model is performing correctly. It should also be emphasized that it is the velocity overshoot that has to be reproduced by the model and not the exact velocity profile since the analytical solution, as stated earlier, is based on an invariant eddy viscosity.

Figure 4.5 shows model reproduction of the velocity overshoot obtained by method A. Model results obtained by employing method B are presented in figure 4.6. As can be seen from figure 4.6 the model fails to reproduce the velocity overshoot by employing method B. It becomes quite evident that the model, employing method A, has qualitatively shown its capability to reproduce the physical processes obtained by analytical solutions and can be supported by experimental evidence. Again, one may further conclude that model assumptions used to obtain the previous results are quite reasonable. On the other hand, results obtained by utilizing method B were not as successful.

Many authors have concluded that in all practical applications eddy viscosity cannot be invariant with time nor with depth (Blumberg, 1975; Elliott, 1976). Figures 4.7 and 4.8 are the instantaneous eddy viscosity profiles at one location at different times throughout a tidal cycle obtained by method A. It is evident from these plots that the

eddy viscosity is indeed a function of time and distance from the bottom boundary. One should also note that in open channel flow, eddy viscosity should attain higher values near a solid boundary (figure 4.9). This can be explained by the fact that eddy viscosity is dependent on the amount of turbulent kinetic energy available. In this case, the primary source of turbulent energy is near the bottom where friction forces dominate. On the other hand, employing method B, figure 4.10, does not show a similar feature that would be expected to exist.

Figures 4.11 and 4.12 present turbulent kinetic energy per unit mass obtained by methods A and B, respectively. These figures show that near the bottom the concentration of energy produced by frictional forces is highest and decrease with distance from the bottom. The same conclusion can be drawn for  $\epsilon$ , the concentration of energy dissipation, profiles. These profiles provide additional support that the model is performing according to theoretical expectations. The same shape of these profiles was obtained by, Alfrink and Rijn (1983).

In order to assure that model calculations are correct, a comparison should be made against an analytical solution or experimental measurements. According to Fischer et al. (1979) the vertical mixing coefficient can be calculated by means of velocity profiles. He showed that by averaging over the total depth, one can calculate eddy viscosity, for a steady open channel flow, as follows:

$$\mathcal{V}_t = 0.067 H U_* \quad (4-17)$$

He also concluded that similar results can be found in a wide range of flows, for example Csanady (1964). Table 4-I contains results obtained by employing the above formula together with the results obtained by

method A and B. One should note that method A underpredicts eddy viscosity while method B overpredicts values obtained by equation (4-3).

For an open channel flow the rate of energy dissipation,  $\epsilon$ , is related to the energy slope,  $S_o$ , as stated earlier by equation (4-11). Table 4-II contains results calculated by employing equation (4-11) as well as model results obtained by employing methods A and B. Rastogi and Rodi (1978) assumed local equilibrium to prevail and showed that energy produced in this case can be calculated via equation (4-15).

Following Rastogi and Rodi (1978), Table 4-II contains values of  $k$  obtained by equation (4-15). Also included in this table are the results calculated by the model when employing methods A and B. One should note that model predictions employing method A underpredicts  $k$  values obtained via equation (4-15). These values are overpredicted if method B is employed.

If tidal forces are introduced to an open channel flow, one should expect that eddy viscosity would attain higher values. This increase in eddy viscosity is the result of higher shear velocities and hence, higher production of turbulent kinetic energy. Model results obtained by either method also show a similar increase when tidal forces are included.

Thus far, results obtained from employing the two methods can be summarized:

#### Method A

- 1- Qualitatively, this method is capable of reproducing the physical processes existing in homogeneous channel flow.

- 2- Quantitatively, this method underpredicts  $\epsilon$ , eddy viscosity and turbulent kinetic energy values obtained by equations (4-11), (4-17) and (4-15).
- 3- This method reproduces the same eddy viscosity profile as that observed in laboratory experiments and practical applications.

#### Method B

- 1- This method qualitatively shows fair agreement with all tests done thus far but not as well as method A.
- 2- This method overpredicts values obtained with equation (4-17) and (4-15) but agrees with energy dissipation values calculated by equation (4-11).
- 3- Finally, this method does not reproduce the proper profile of eddy viscosity in the vertical direction.

Some discrepancies have arisen when model results were compared with analytical solutions. When employing method A, one could adjust the constant  $C_\mu$  in equation (2-30) to 0.20 instead of 0.09. This would lead to a very good agreement with values obtained from equation (4-17) and (4-15) as can be seen from table 4-III. Calculations for energy dissipation obtained from method B are in a good agreement with analytical results, but overpredictions exist in the calculation of eddy viscosity and turbulent kinetic energy. Additionally, method B failed to reproduce the velocity overshoot near the bottom boundary as predicted by the analytical solution. After weighting the shortcomings of both methods, method A was adopted after adjusting the value of  $C_\mu$  to 0.20.

### C. Model verifications in a continuously stratified flow

In this section an attempt is made to test the standard  $k-z$  model in a non-homogeneous flow. This requires the introduction of buoyancy forces in the momentum and the energy balance. Buoyancy effects are included in the 'G' term as defined in equation (2-29a).

The final integrated form of the G term, according to the Mean Value Theorem, is

$$G = \beta g \nu_t [ S_{top} - S_{bot} ] / (\sigma_t \Delta z) \quad (4-18)$$

The above term, G, will become a sink under stable stratified conditions, and thus reduce the amount of energy available for mixing. Since buoyancy production must be reduced, then diffusivity of salt,  $\nu_t$ , must also be reduced. In unstable stratification, the same term will act as a source, allowing energy to grow and forcing the water column to become homogeneous.

Gibson and Launder (1978) have concluded that the buoyancy term appearing in the  $\epsilon$  equation has little or no effect on the rate of energy dissipation. It should be noted that the G term in the  $\epsilon$  equation is multiplied by a factor,  $\epsilon/k$ . An order of magnitude analysis shows that, under very highly stratified conditions, this factor is indeed very small. In turn, this ratio,  $\epsilon/k$ , will force the buoyancy term to become much smaller than all other terms in the  $\epsilon$  equation.

In model calculations employing either method A or B, the primary source of turbulent kinetic energy or its dissipation is located near the bottom. Turbulent kinetic energy is transported to upper layers by diffusion processes. If the numerical scheme does not allow the diffusivity of salt to be reduced, due to the stable stratification, then the buoyancy term will dominate. Conversely, the buoyancy term

appears as a sink in all layers. It is apparent that the rate of energy diffusion from the bottom is not the same order of magnitude as the buoyancy term as will be seen in the following section. In this case, the diffused energy,  $k$ , will become much smaller than the buoyancy term. This will result in a negative turbulent kinetic energy concentration which is impossible, physically incorrect and hence, a quantitative calculation can not be made. In order to show that the buoyancy term is predominant it is necessary at this point to estimate the order of magnitude of each term appearing in the  $k$  equation (3-14). In arriving at such an estimate the following model parameters were used as well as equation (4-15).

$$\Delta z = 200 \text{ cm}$$

$$k = 0.022 \text{ cm}^2 / \text{sec}^2$$

$$\Delta S = S_{\text{bot}} - S_{\text{top}} = 1 \text{ ppt}$$

$$\Delta U = U_{\text{top}} - U_{\text{bot}} = 2 \text{ cm} / \text{sec}$$

$$e = 2 \times 10^{-6} \text{ cm}^2 / \text{sec}^2$$

$$V_t = 10 \text{ cm}^2 / \text{sec}$$

If horizontal transport of  $k$  is neglected, then equation (3-14) can be written as follows

$$\frac{\partial k}{\partial t} = \frac{\partial}{\partial z} \left( \frac{V_t}{\sigma_k} \frac{\partial k}{\partial z} \right) + V_t \left( \frac{\partial U}{\partial z} \right) \frac{\partial U}{\partial z} + \beta g \frac{V_t}{\sigma_t} \frac{\partial S}{\partial z} - e \quad (4-19)$$

substituting the above model parameters results in the following estimates

$$\frac{\partial k}{\partial t} = 6 \times 10^{-6} + 1 \times 10^{-3} - 3 \times 10^{-3} - 2 \times 10^{-6}$$

It is quite evident from the above estimates that the buoyancy term is an order of magnitude larger than the production and diffusion terms combined. This, as stated earlier, results in negative energy and hence

no model run can be made. Another alternative is to change the value of  $\sigma_k$  in order to increase the rate of energy diffusion. This would result in an incorrect energy profile, and did not solve the problem.

In equation 4-19 when  $k$  goes to zero, then all terms and the eddy viscosity also go to zero. Theoretically equation 4-19 as written can not generate a  $k$  less than zero. On the other hand, the numerical scheme employed with a finite value of  $k$  can obtain a negative  $k$  value and the buoyancy term dominates. In order to solve this problem, the numerical scheme should calculate eddy viscosity at the new time step rather than the previous time step. The numerical scheme employed herein does not allow for this, and hence a negative  $k$  value is reached. Additionally, although the numerical scheme solves the  $k$  equation implicitly in the vertical direction, the source and the sink terms, e.g. production by shear stress and destruction by buoyancy, are solved explicitly. This time constraint is stringent and also hard to assess. The time step used with the numerical scheme was less than 100 seconds.

The  $k$ - $\epsilon$  model was originally intended to be used to simulate gravitational circulation in the James River Estuary. The primary reason for selecting this study site is the availability of data for this river. From this data base, one can estimate the order of magnitude for each term appearing in equation (3-14).

The average depth of the James River Estuary is about 10 meters. Typical top to bottom salinity difference is about 4 ppt. From tide-tables the average tidal velocity was found to be 50 cm/sec. Pritchard (1960) has found that eddy viscosity in the James River Estuary ranges from 1 to  $10 \text{ cm}^2/\text{sec}$ . A  $10 \text{ cm}^2/\text{sec}$  value is used. Pritchard (1960) also showed that, the vertical velocity gradient can be represented as

0.7 WII. Substituting the preceding values into equation (3-14) will result in the following estimates.

$$\frac{\partial k}{\partial t} = 2 \times 10^{-4} + 1.2 \times 10^{-3} - 3 \times 10^{-3} - 8 \times 10^{-4}$$

One should note that if an interior layer is considered then the production term is one or two orders of magnitude smaller than the above estimate. In order to rectify this problem several approaches have been taken as described.

For a stratified flow, momentum and mass fluxes are much smaller than their counterparts in homogeneous flow. This is a well known fact and has been observed in many estuaries (Fisher et al., 1979). Since no model run can be made as proposed, one should search for a different solution. The approach employed by Cerco (1982) and Kuo et al. (1978) to reduce turbulent fluxes from homogeneous to non-homogeneous flow in the mixing length hypothesis is adopted here. In this approach, a functional form of the Richardson number can be employed. This functional form has been derived in such a way that when no stratification exists the original form is obtained. For example, one can adopt the following :

$$D_t = D_{t_0z} / (1 + R_i) \quad (4-20)$$

in which

$D_{t_0z}$  = eddy viscosity in homogeneous flow

$$R_i = - \frac{g}{\rho} \frac{\partial \rho}{\partial z} / \left( - \frac{\partial U}{\partial z} \right)^2 \quad (4-20a)$$

In this case, one should neglect the buoyancy in the  $k$  equation for reasons stated earlier. In addition, eddy diffusivity can be reduced by a similar function

$$\Gamma = \nu_t / (1 + R_i) \quad (4-21)$$

In order to make the standard  $k$ - $\epsilon$  model work the solution lies within two key points. First, from a review of literature, it is evident that the Schmidt/Prandtl number, or Reynolds analogy, still raises a big controversy over its correct value. This number normally falls between 0.5 to 5, a considerable range. To overcome this problem, one could either solve an extra equation to account for turbulent fluxes or employ a constant value which best fits the data. Another approach is to adopt a functional form that reduces turbulent fluxes and hence accounts for stratification effects. Secondly, the proposed constant appearing in equation (2-30) could be changed to a function similar to equation (4-21). In brief, the two functions could be thought of as follows

$$C_\mu = C_{\mu_0} / (1 + a R_i)^b \quad (4-22)$$

$$\sigma_t = \sigma_{t_0} \times (1 + c R_i)^d \quad (4-23)$$

in which

$C_{\mu_0}$  = value for neutrally buoyant flows.

$\sigma_{t_0}$  = value for neutrally buoyant flows.

In equations (4-22) and (4-23),  $a$ ,  $b$ ,  $c$  and  $d$  are constants which can only be determined by trial and error, the combinations for a solution could be limitless. Results using the above set of equations were unsatisfactory because eddy viscosity were very high and resulted in a homogenous water column

### Summary

The k-ε model can be applied to a nonbuoyant channel flow if an adjustment is made to the constant  $C_{\mu}$  in equation (2-30). It is then that model results can be legitimately compared with those obtained experimentally or by analytical solutions.

At this stage, a brief description of some of the trials that have been made in an attempt to realistically apply the k-ε model for stratified flow condition is in order:

- 1- Neglect G in the k equation and apply equation (4-20) and (4-21).
- 2- Include G and employ equations (4-22) and (4-23).
- 3- Repeat steps 1 and 2 with an  $R_f$  dependency instead of  $R_i$ .
- 4- Employ a constant with a somewhat larger  $\sigma_k$  value than was suggested by Reynolds.
- 5- Add a production term to each layer, varying width, and including G.

All of the above attempts to account for stratification effects by the standard k-ε model are the result of this extensive and lengthy study. None of the above attempts resulted in a successful simulation of a stably stratified flow.

It should also be stated that the main reason for the failure of the standard k-ε model is due to the buoyancy term. If horizontal transport of energy is neglected then the k equation can be written as follows

$$\frac{\partial k}{\partial t} = \frac{\partial}{\partial z} \left( \frac{\nu_t}{\sigma_k} \frac{\partial k}{\partial z} \right) + \nu_t \left( \frac{\partial U}{\partial z} \right)^2 (1 - R_f) - \epsilon \quad (4-24)$$

For stable stratification  $R_f$  approaches the critical value and hence, reduces the buoyancy term. In the standard model the production terms become small as  $R_f$  approaches 1. The standard model incorporates no critical  $R_f$  but does allow  $k$  to decrease as  $R_f$  increases which may lead to numerical instability in the calculation. What is more desirable is for eddy viscosity to approach zero as  $R_f$  goes to  $R_{fc}$ ; which leads to a realistic incorporation of the effects of stratification and would also stabilize the numerical scheme since the buoyancy production would never be greater in absolute magnitude than the shear production for  $R_f < 1$ . However, there is a general agreement that the critical  $R_f$  is significantly less than 1 with values in the range 1/6 to 1/4 being reported. The  $k-\epsilon$  model does not account for the reduction in mixing at these lower values of  $R_f$ 's. Therefore, the buoyancy term remain unaffected and hence, dominates the  $k$  equation.

After employing every logical approach, it is the author's opinion that the standard  $k-\epsilon$  model, as proposed by Rodi (1980a), can not be applied to a stratified flow condition in which buoyancy has a pronounced effect. The same conclusion has also been reached by Rodi (1987).

Table 4-I : Eddy viscosity estimates by method A and B.

Table 4-II : Estimates of energy and its dissipation by  
method A and B.

Table 4-III : Estimates of eddy viscosity, energy and its  
dissipation by method A.

Table 4-I  $C_u = .09$

	$\bar{v}_c \frac{cm^2}{sec}$
Eq. 4-17	11.4
Method A	4.8
Method B	34.6

Table 4-II  $C_u = .09$

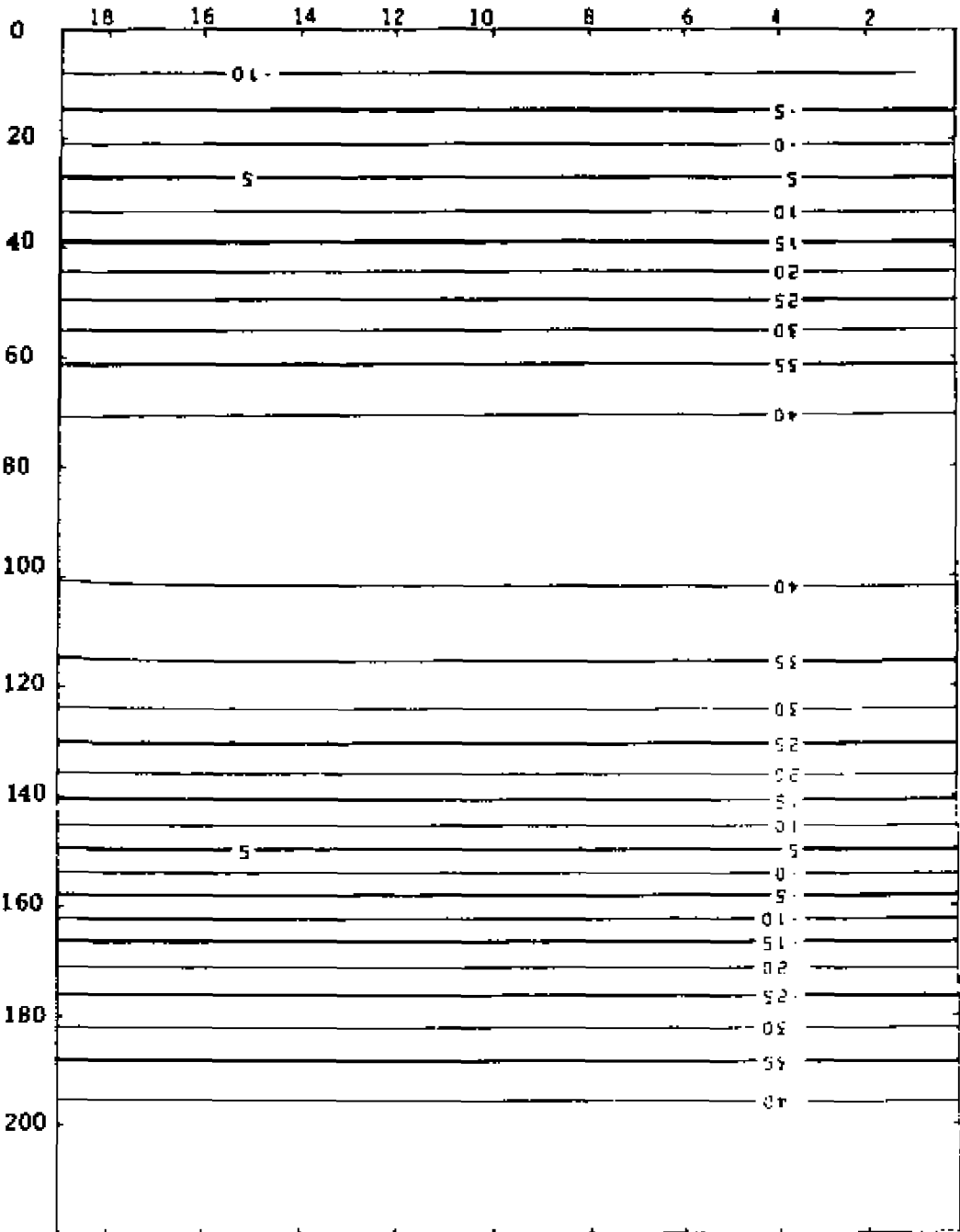
	$\bar{k} \frac{cm^2}{sec^2}$	$\bar{\epsilon} \frac{cm^2}{sec^3}$
Eq. 4-18 & 14	.024	.000018
Method A	.012	.000004
Method B	.075	.00002

Table 4-III  $C_u = .20$

	$\bar{v}_c \frac{cm^2}{sec}$	$\bar{k} \frac{cm^2}{sec^2}$	$\bar{\epsilon} \frac{cm^2}{sec^3}$
Eq. 4-17	11.4	.021	.000018
Method A	14.5	.024	.000081

Figure 4.1 : Velocity contours in an open channel; friction forces are not included method A

DEPTH (METER)



Velocity contours are in cm/sec

TIME (TIME STEPS)

Figure 4.2 : Velocity contours in an open channel; friction forces are not included method B

DEPTH (METER)

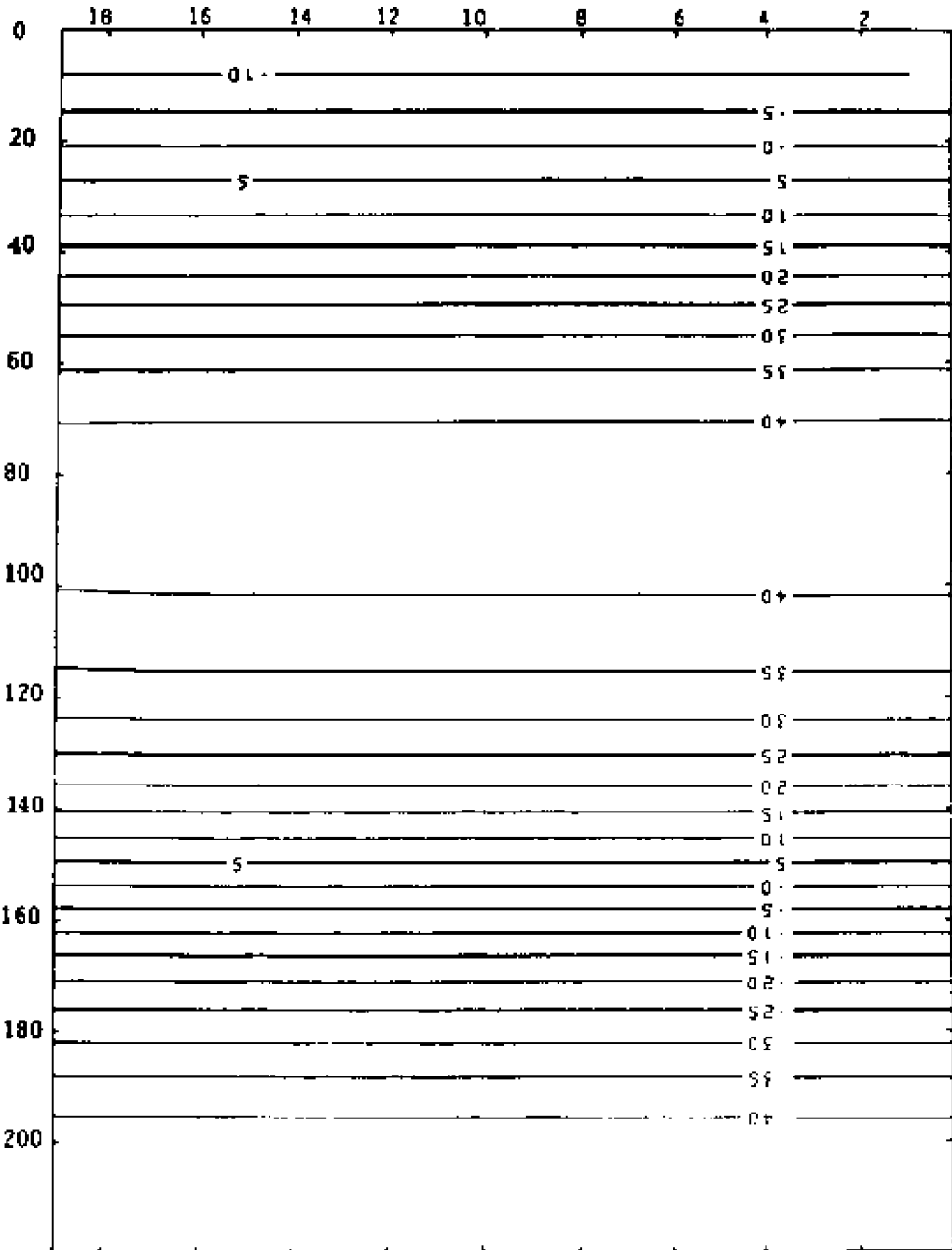


Figure 4.3 : Velocity contours in an open channel; friction forces are included method A

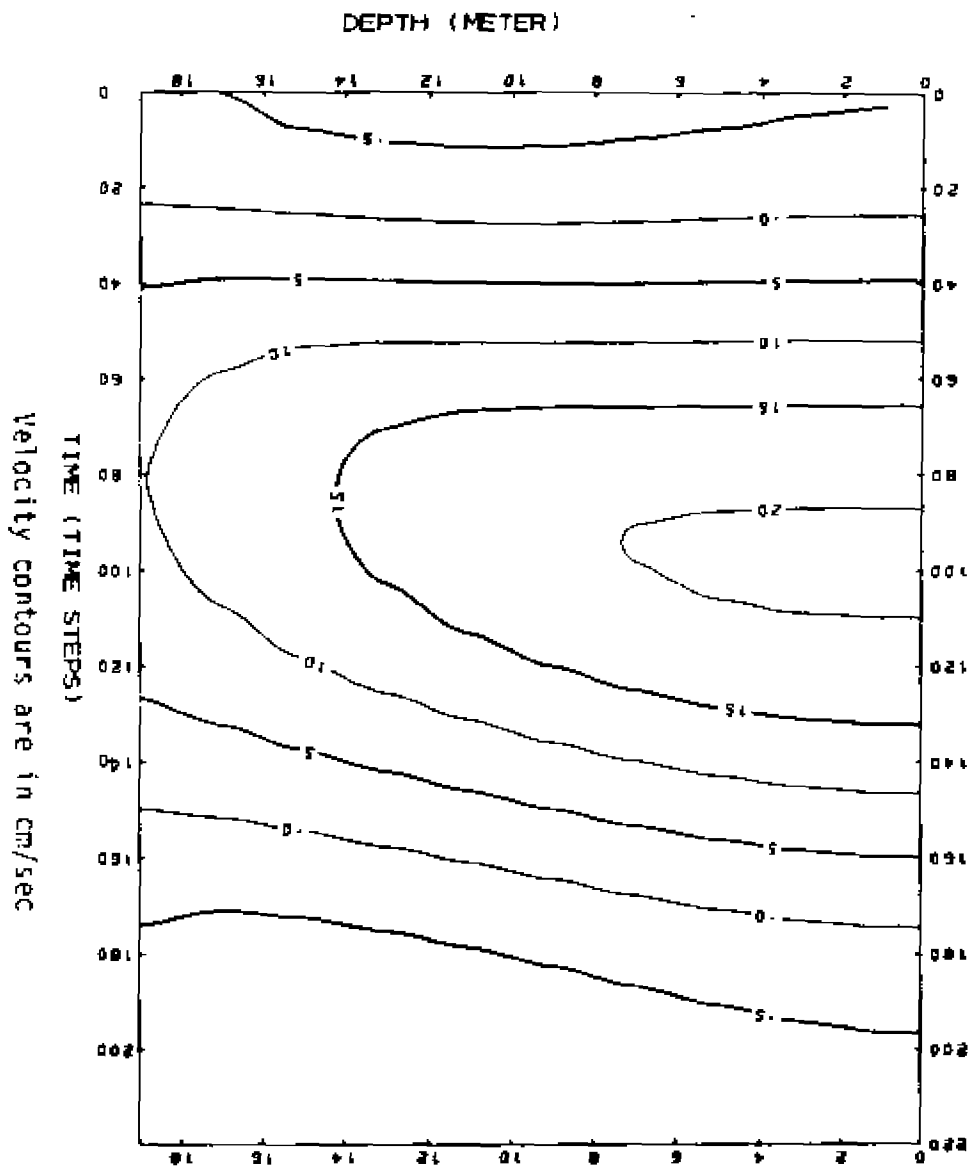
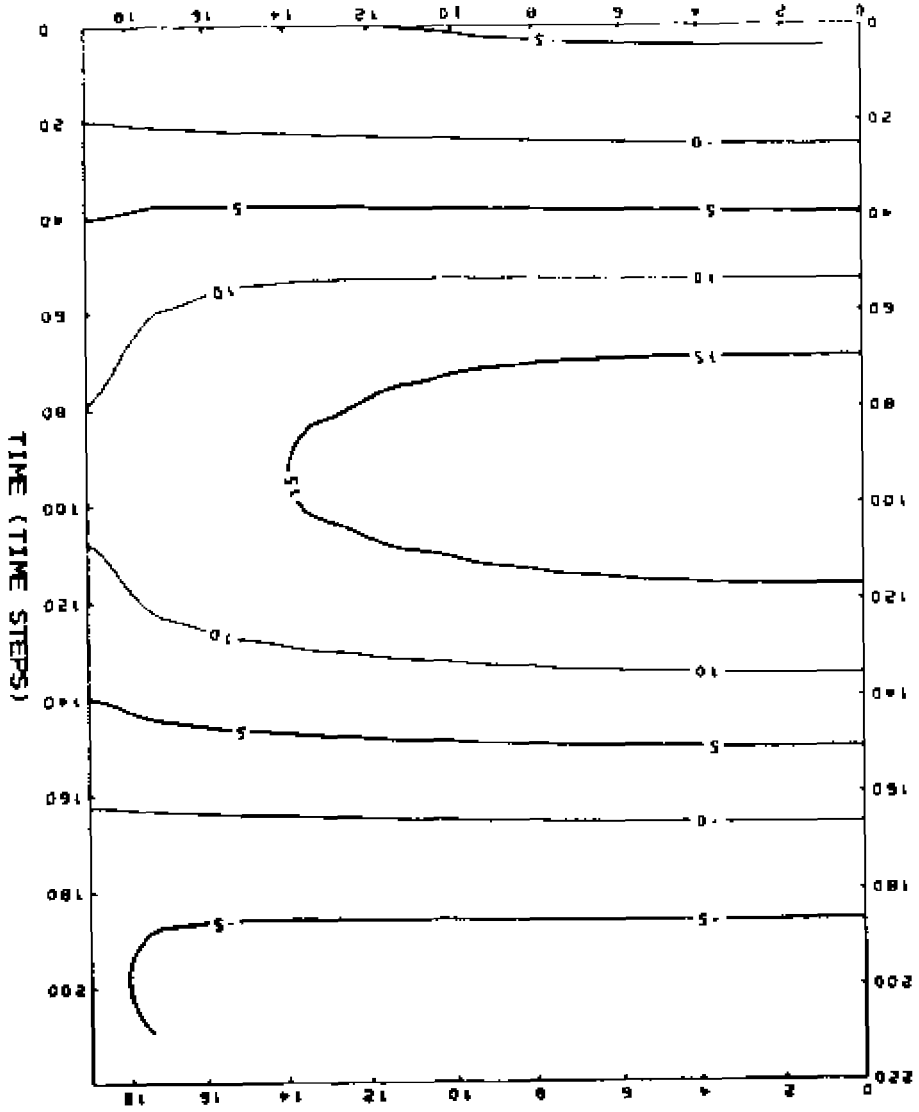


Figure 4.4 : Velocity contours in an open channel; friction forces are included method B

DEPTH (METER)



Velocity contours are in cm/sec

Figure 4.5 : Velocity overshoot near a rough bottom method A

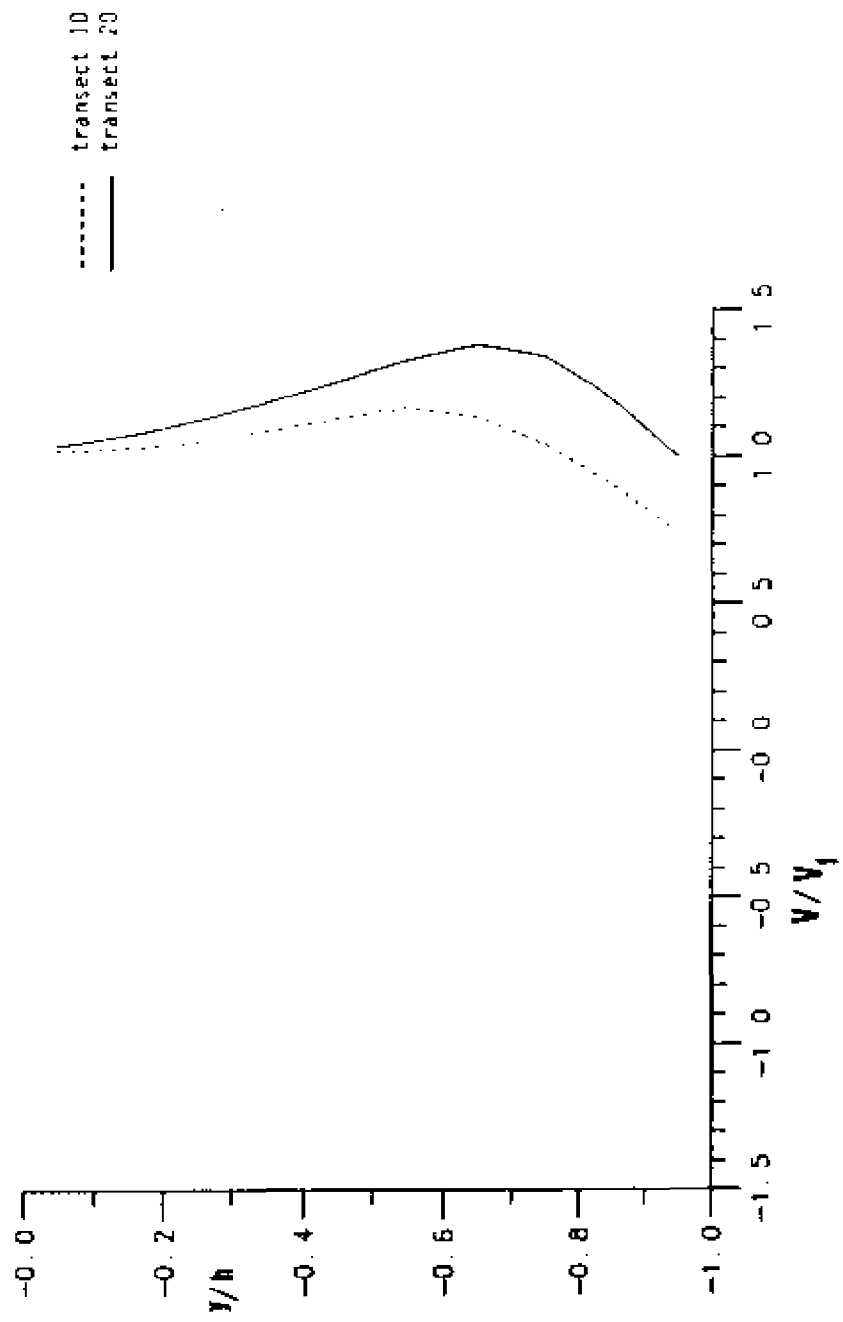


Figure 4.6 : Velocity overshoot near a rough bottom method B

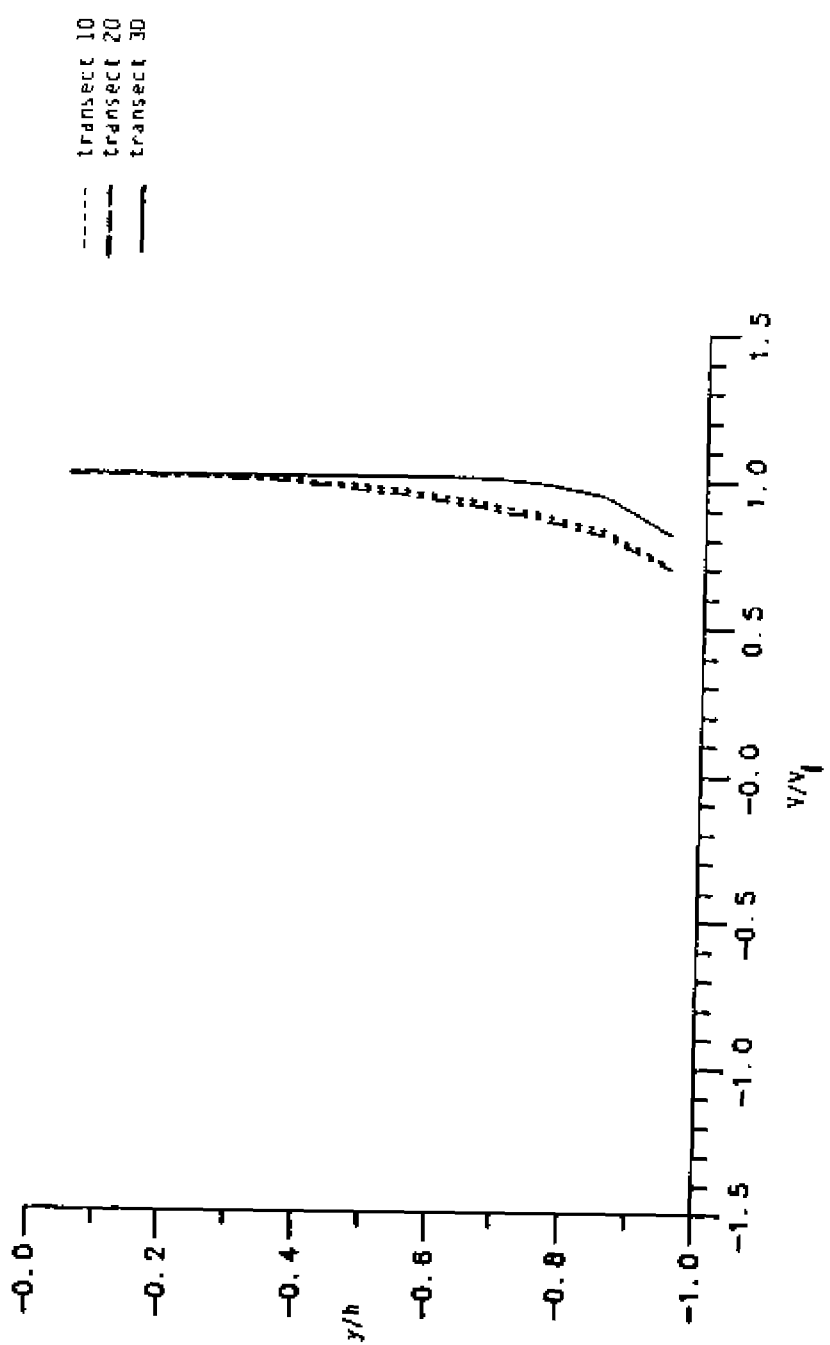


Figure 4.7 : Instantaneous eddy viscosity profiles at  
different times within one tidal cycle at a  
specific location method A

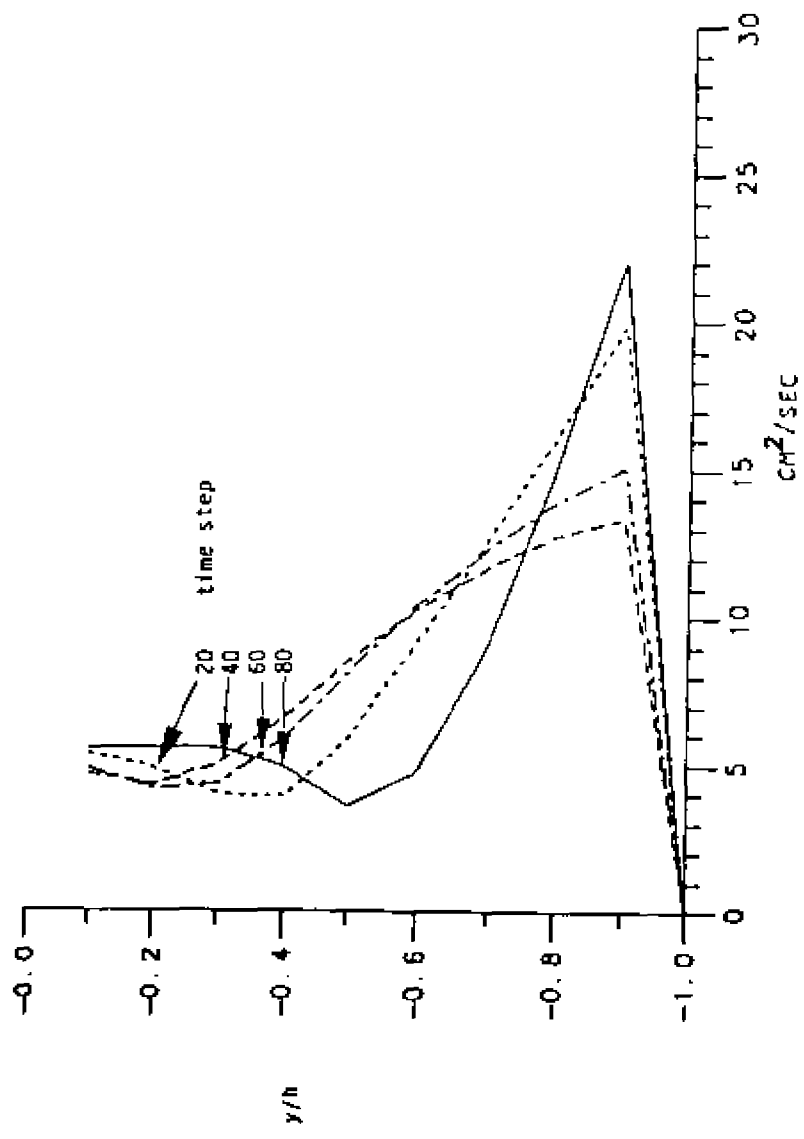


Figure 4.8 : Instantaneous eddy viscosity profiles at different times within one tidal cycle at a specific location method A

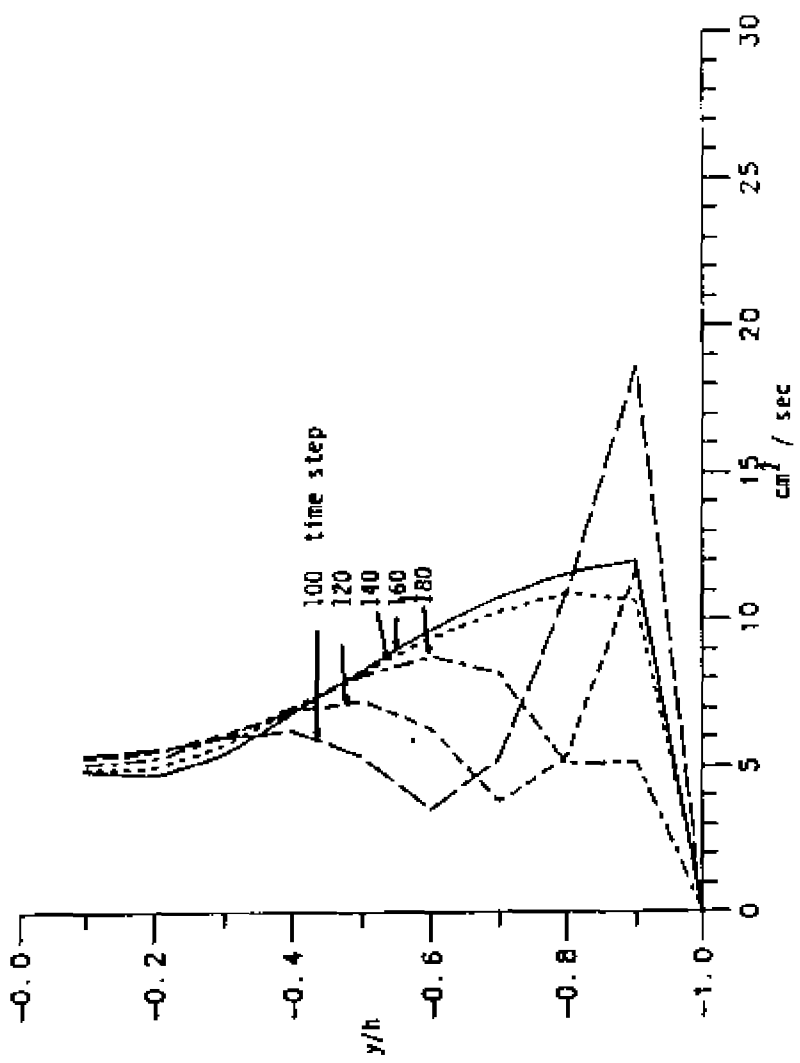


Figure 4.9 : Tidal-averaged eddy viscosity profiles at  
different locations along the channel method A

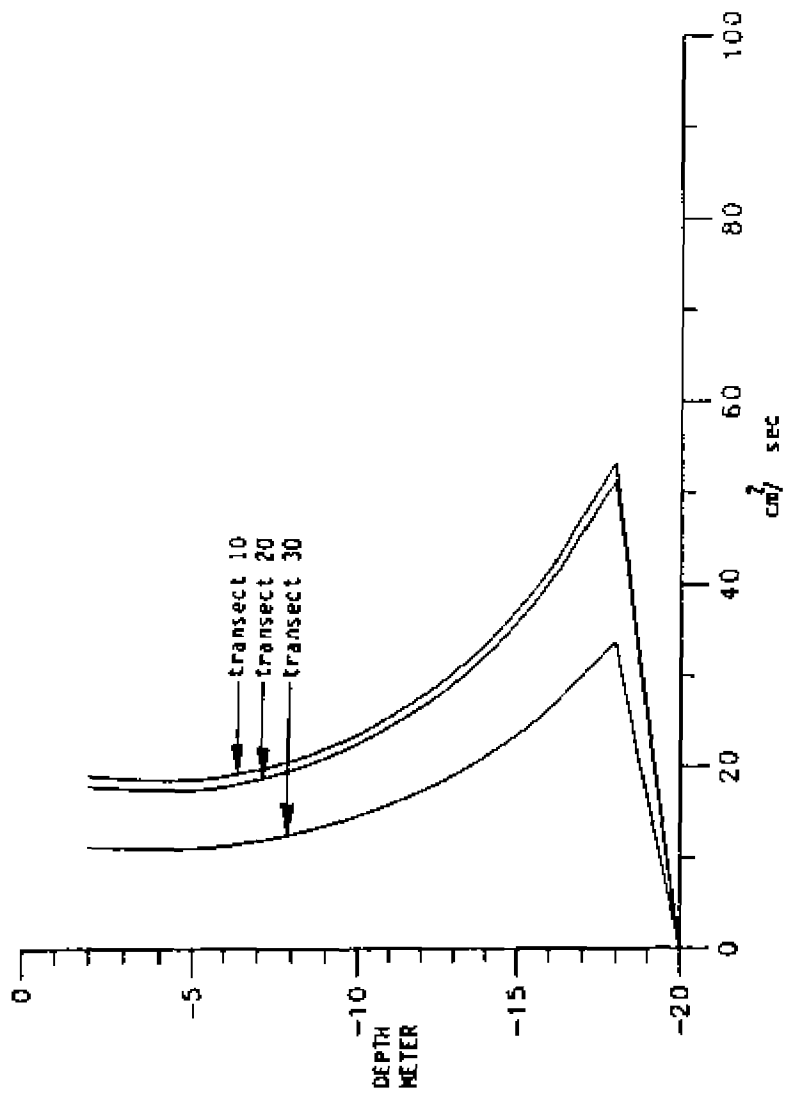


Figure 4.10 : Tidal-averaged eddy viscosity profiles at  
different locations along the channel method B

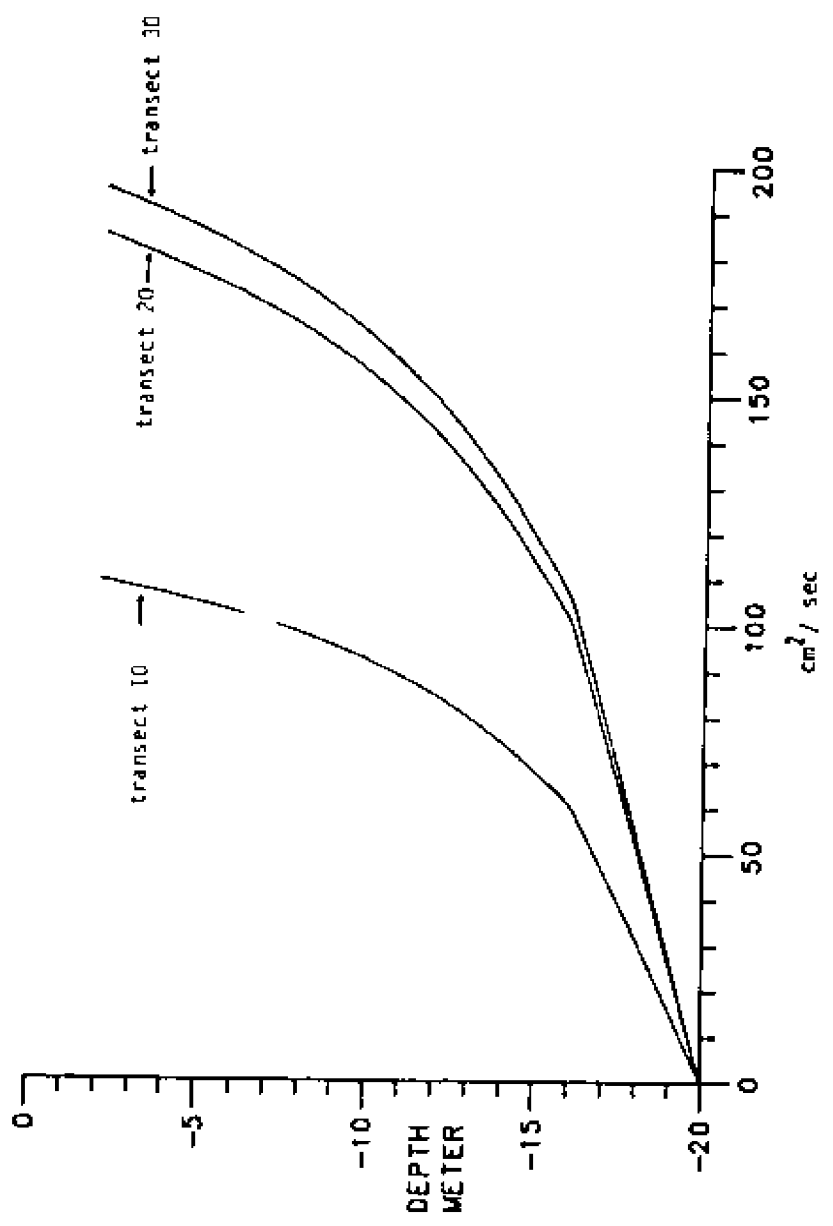


Figure 4.11 : Tidal-averaged energy concentration profiles at  
different locations along the channel method A

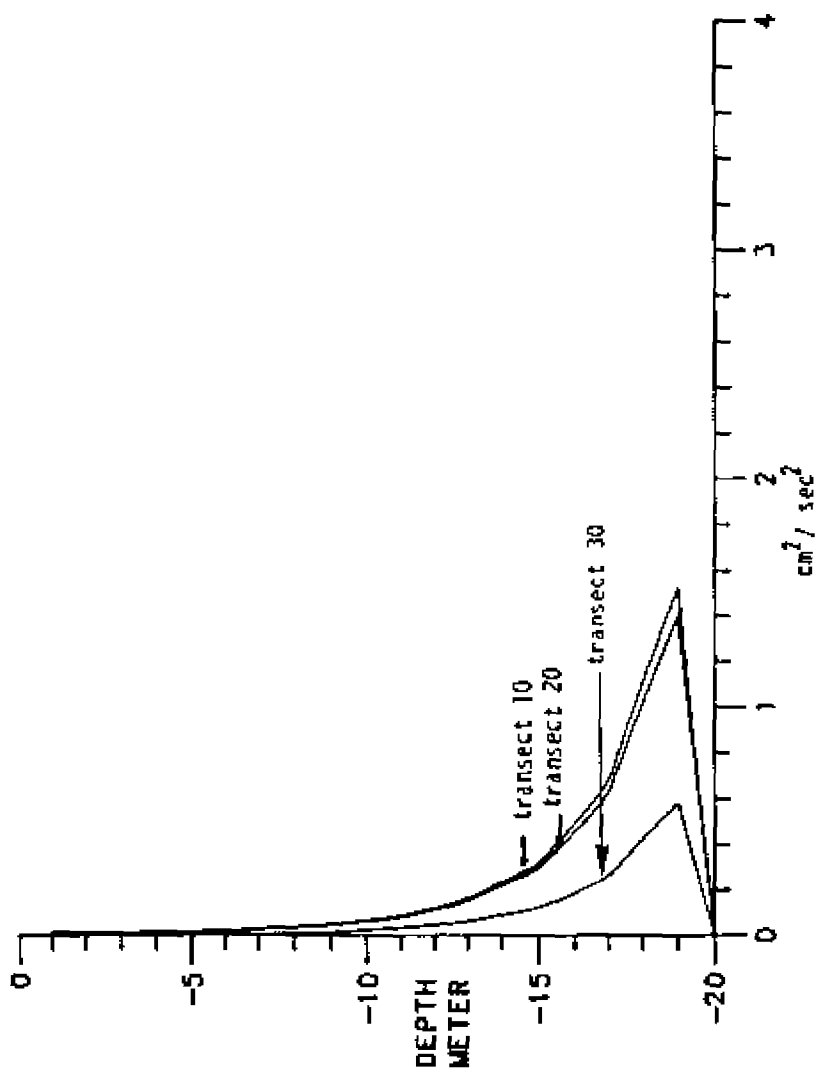
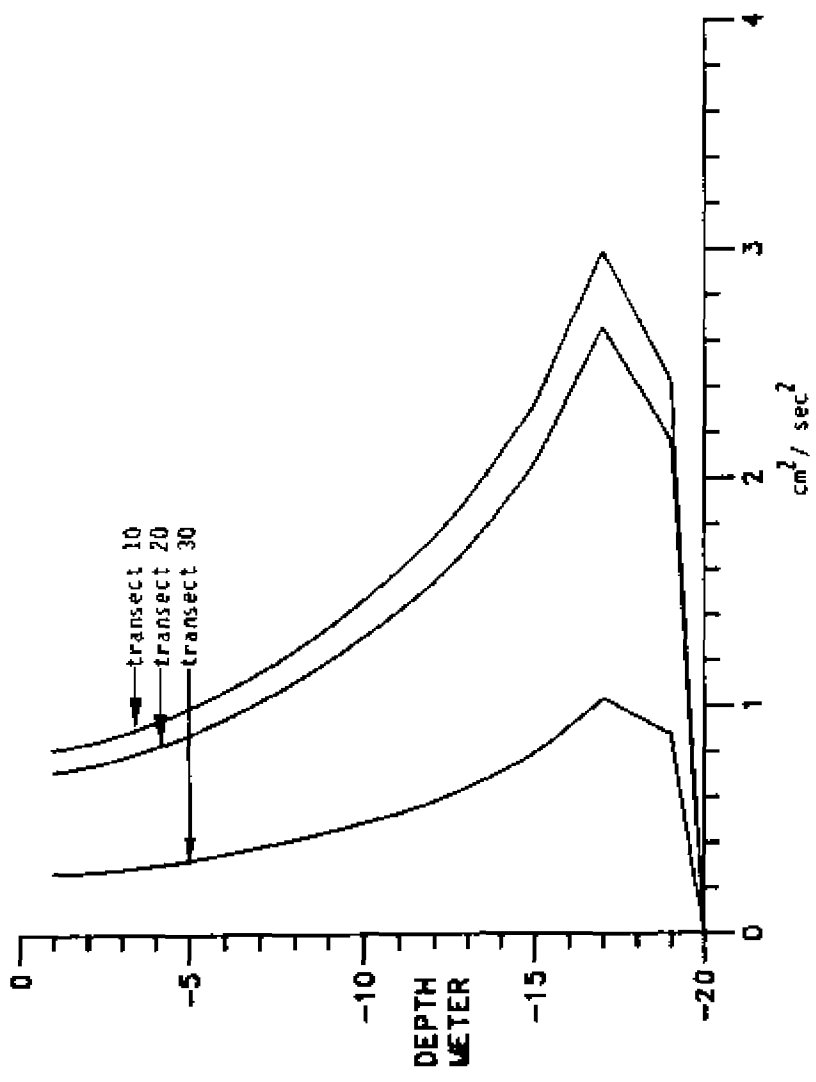


Figure 4.12 : Tidal-averaged energy concentration profiles at  
different locations along the channel method B



## CHAPTER V.

### VERIFICATIONS AND APPLICATIONS OF THE LEVEL TWO MODEL

Since chapter 4 is devoted to the k- $\epsilon$  model, this chapter is exclusively oriented towards the verification of the level two model. In order to make a proper comparison between the two closure schemes selected for this study, the level two model was subjected to all tests that have been previously applied to the standard k- $\epsilon$  model. For example, in section A, model results employing level two as a closure scheme are tested against the analytical solution and experimental results obtained by Knight and Ridgeway (1976). The applicability of the level two model to a nonbuoyant open channel flow, is discussed and compared with experimental results in section B. The final section, C, is devoted to comparing level two model results with laboratory experiments.

#### A. Model verifications in a nonbuoyant channel flow

Knight and Ridgeway (1976) have shown that there exists no phase lag between surface and bottom velocities in a two-dimensional frictionless homogeneous open channel flow. The mathematical model employing the level two model as a closure scheme has been employed to simulate such conditions. Parameters used in this run are identical to parameters employed in the k- $\epsilon$  model in the previous chapter. It should

be emphasized that a small Manning's coefficient, as stated in chapter 4, is employed to simulate the frictionless case runs. Model results for this run are shown in figure 5.1. In this figure the x axis presents time for one tidal cycle and the y axis presents channel depth. From figure 5.1, it is apparent that the model and the analytical solution are in excellent agreement. It can be seen that there exists no phase lag between surface and bottom velocities.

If such a channel is subjected to friction forces, then the analytical solution will lead to a non-zero phase difference between surface and bottom velocities. Model results for an open channel flow with friction and tide are shown in figure 5.2. In this figure, it may be noted that bottom velocity reaches slack before flood or ebb earlier than surface velocity. Ippen and Harleman (1966) have shown that a phase lag exists between surface and bottom velocities and have been verified in various laboratory experiments (i.e. Knight and Ridgeway, 1976).

As previously stated in Chapter 4, an analytical solution can be obtained for this channel assuming an invariant vertical eddy viscosity. Since eddy viscosity has been shown to be depth and time dependent, no comparison should be made. Following Fischer et. al. (1979) eddy viscosity can be estimated by equation (4-17). Table 5-1 contains results obtained by this equation along with model predictions by both the level two and the mixing length models. Several model runs were made employing the mixing length hypothesis as a closure scheme to determine the constant value required for equations (5-2) and (5-4). These values are as follows

$a = 0.5$ , and

$$\alpha_1 = 1.0$$

It should be noted here that the level two model does not require such procedure. Results obtained by the level two model are slightly higher than those obtained by equation (4-17). These higher values are not significant when one considers that no further tuning is required. On the other hand, the mixing length model is comparable to equation (4-17). These results, as stated earlier, were obtained by tuning the model for such an application.

If tidal forces are introduced to an open channel flow, one should expect that eddy viscosity would attain higher values. This increase in eddy viscosity is the result of higher shear velocities and hence, higher production of turbulent kinetic energy. Results obtained by either method also show a similar increase when tidal forces are included.

#### **B. Model verifications in a continually stratified flow**

Harleman and Ippen (1967) studied one- and two-dimensional salinity intrusions in a physical model. Their study was conducted in a horizontal, rectangular flume 100 meters long and 0.229 meters wide. Average water depth in the flume was 15.1 cm. At the closed end of the flume freshwater was introduced at a controlled rate and at the opposite end the flume was connected to a tidal basin of constant salinity where a simple harmonic tide was maintained. Such an investigation would provide the necessary information to further verify the model employed in this study. Measurements of salinity and velocity along the flume and perpendicular to the main flow direction were made at several stations. In the following section an attempt is made to simulate

experiment 16 described in Ippen and Harleman (1966) using level two model. Table 5-I contains parameters employed for this model run.

In order to simulate the flume runs, the channel was divided into 30 longitudinal transects 3.33 meters apart. Channel depth was divided into 5 equally spaced layers 3.0 cm thick. A 10 second time step was employed for this simulation.

Table 5-I, Flume Parameters Experiment # 16

Channel length = 100 meters	Tidal Amplitude = 1.5 cm
Channel Depth = 15.1 cm	Tidal Period = 600 secs
Freshwater Input = 200 cm <sup>3</sup> /sec	Basin Salinity = 29.2 ppt

#### B-1 Model calibration

In order to make the proper simulation, the numerical model should first be calibrated. Calibration can be achieved by running the numerical model with different Manning's coefficients until agreement is obtained with observed tidal amplitudes along the channel. Experiment 29 (Ippen and Harleman, 1961) provided the necessary information to calibrate the model. Best agreement was obtained by employing a Manning's n of 0.024. Model results plotted against flume tidal amplitudes are shown in figure 5.3. Both model results and flume data are in very good agreement.

Longitudinal dispersion due to transverse velocity shear was calculated using Taylor's formula. The following equation was employed.

$$K_x, N_x = 20 R U_* \quad (5-1)$$

in which

R = Hydraulic radius of channel

$U_*$  = shear velocity

For a numerical model employing the mixing length hypothesis, constants needed for the functional form are obtained by running the model with different values until agreement is obtained with the flume data. In contrast, for the level two model this is unnecessary. The cited values for the constants employed in Mellor and Yamada (1982) are used. No further adjustment to these constants are required. These values are

$$A_1, B_1, A_2, B_2, C_1 = (0.78, 0.78, 15.0, 8.0, 0.056)$$

Several expressions can be used to calculate the characteristic mixing length scale. The following equation is used for this study

$$L = k' \frac{z}{H} \left( 1 - \frac{z}{H} \right)$$

in which

$k'$  = Von Karman constant (taken as 0.40)

$z$  = Distance from boundary

$H$  = Total depth

Ippen and Harleman (1961) ran the flume data for twenty tidal cycles for most experiments, after which measurements were made.

The tidal-averaged longitudinal and vertical salinity distributions, normalized by basin salinity, for flume experiment number 16 are shown in figure 5.4 and 5.5. Model results for the same run are indicated by the broken lines. The numerical model shows very good agreement in predicting the extent of the salt intrusion. As can be seen in these figures, model results are also in good agreement in predicting vertical salinity distributions. One should note the

disparity at station 80. Model results at this station indicate less stratification.

Model results for the tidal-averaged horizontal and vertical velocities are shown in figures 5.6 and 5.7. Experimental results for these variables are also plotted in figures 5.6 and 5.7. It is evident that the model reproduced the two layer circulation pattern as shown in figure 5.6. However, model results indicate lower velocities than laboratory results. The main reason for such discrepancies is the fact that flume measurements were made from the center of the channel. Such measurements tend to be higher than the width averaged velocities. Since model predictions of horizontal velocities are less than those obtained from flume data, and since vertical velocities are calculated by the same principle of continuity, one should expect that the numerical model will also tend to underestimate vertical velocities. Thus far, the level two model has proven to predict to a reasonable extent, most physical processes in buoyant and non-buoyant flows. Model results have shown a good agreement when applied to a continually stratified flow. One should note that all these tests have been performed with the same set of constants cited from Mellor and Yamada (1982). A comparison between the level two model and models employing the mixing length hypothesis is in order. The primary purpose for such a comparison is to evaluate the performance of each model in these applications.

### C. Comparison of models employing level two and M.L.H for closure

In this section models employing the level two and the mixing length hypothesis as a closure scheme will be compared. The performance of these two schemes in a continually stratified flow is chosen as a bench mark for comparisons. Cerco (1982), employed the mixing length hypothesis as a closure scheme in a study of the James River Estuary. In order to verify his model, a simulation of Harleman and Jppen (1967) flume experiment number 29 was made. Results of this simulation are shown in figures 5.6 and 5.7. Cerco chose the following forms to calculate eddy diffusivity

$$\Gamma_0 = a u \quad (5-2)$$

in which

$\Gamma_0$  = eddy diffusion coefficient in a non-stratified flow

$a$  = 0.085 cm

$u$  = instantaneous velocity.

In order to account for stratification effects a generalized form was adopted for his study as written below

$$\Gamma = \frac{\Gamma_0}{(b + c R_i)^n} \quad (5-3)$$

in which

$R_i$  = local Richardson number

$b, c, n$  = empirical constants = 1.0 for flume comparison,

and for eddy viscosity a linear relationship is assumed as follows

$$\mathcal{V}_t = \sigma_t \Gamma \quad (5-4)$$

in which

$\sigma_t$  = 1.0 for flume data comparison.

Evaluation of these constants was accomplished by trial and error. Series of model runs were made until tidal-averaged eddy diffusivity fell within the range reported by Harleman and Ippen (1967). On the other hand, the level two model for the same experiment did not require such a procedure. As stated earlier, the constants needed for this model were obtained from Mellor and Yamada (1982). There was no further tuning required for these constants. It should be emphasized that, for inexperienced users the procedure of tuning the model for a specific application could be cumbersome. Therefore, concerning the applicability of the model, it is evident that the level two model is easier to apply than the mixing length formulae.

Both models, the level two and the mixing length model, with the numerical scheme adopted herein are equally feasible for long time simulations. The semi-implicit method chosen for the two models allows for a much longer time step than required by other methods. Therefore, long-time simulation appears to be less expensive when compared with other methods.

Comparison between the two schemes will be performed in three steps. The first step is to compare the salinity distribution. Secondly, the horizontal velocities are compared and finally the vertical velocities.

### **C-1 Salinity distribution**

For Harleman and Ippen's flume data, the length of the salt intrusion is defined as 1% of the basin salinity. Model results obtained by the level two model are shown in figure 5.4 and results obtained by employing the mixing length hypothesis are also shown in

figure 5.4. It is quite evident from these plots that both models predict the length of the salt intrusion extremely well. Agreement between model predictions and flume data for longitudinal salinity distributions is also achieved. Vertical salinity distributions obtained by level two and mixing length hypothesis models are presented in figure 5.5. In this plot, the x-axis is the normalized vertical salinity distribution,  $S/S_0$ , and the y-axis is the normalized depth,  $Y/h$ . Station numbers refer to distance, in feet, from the open boundary. Although the over-all agreement between model results and flume data are encouraging, agreement obtained at station 5 should be viewed cautiously and will be explained later. It should be noted here that model predictions for station 40 obtained from the level two model are less satisfactory. At this station, model results indicate lower stratification than the one observed in the flume data.

#### C-2 Longitudinal velocity distribution.

As a second step, model predictions obtained by level two and mixing length hypothesis for longitudinal velocities will be compared with the measured flume data. Figure 5.6 shows predictions by both models for longitudinal velocities. It can be seen that both models underpredict the horizontal velocity distribution. On the other hand, it should be noted that model results obtained by level two indicate higher velocity values. As previously mentioned, velocity measurements are taken at the center of the channel. These, in turn, tend to have higher values than width averaged velocities. Thus, one should expect that model predictions should be less than observed data. With this,

one can conclude that results of the level two model are in better agreement with observations than the mixing length hypothesis model.

### C-3 Vertical velocity distribution

Vertical velocities are calculated by using the principle of continuity for both models. Therefore, if model results are less than velocity measurements in the horizontal direction, it is anticipated that the vertical velocity will follow suit. In figure 5.7 the vertical velocity distributions, obtained by both models, are shown. It is evident from these plots that the level two model predictions are in better agreement with observations. One should also note that station 5 is omitted from these plots. The reason for this is because both flume and model boundary conditions at the open boundary are not well known. Boundary conditions for the flume data were set as the salinity in the basin and not at the mouth. On the other hand the boundary condition for the model  $\frac{\partial^2 U}{\partial x^2} = 0.0$  is required for closure but is not necessarily the appropriate one at the mouth. Therefore, measurements and predictions by both models at the open boundary should be viewed with caution. One should also note that, results obtained by the level two model are consistent with flume data. Both the flume data and the level two model indicate an increase in the downward velocity between station 80 and 120 and then a decrease between stations 120 and 160. On the other hand, the mixing length model indicates an increase from station 80 to 120 and also 160. These results are not consistent with flume data. Thus, one can conclude that the level two model does show better agreement and consistency with observations than models employing the

mixing length hypothesis. In addition, the level two model does not require a tedious tuning for the constants employed in the model. It also should be noted that a person with good experience in mathematical modeling should do as well employing the M.L.H. A general conclusion can not be drawn at this time. In order to do so both models should be applied to a variety of flow conditions and results obtained should be compared. Then, and only then, can a generalized conclusion be made.

In conclusion, the level two model is superior to models employing the mixing length hypothesis as a closure scheme. The level two model is simple, easy to apply, and does not need as much tuning to the constants employed as the mixing length approach. In addition, model comparisons have shown that the level two model results are more consistent with flume data. Since the level two model and the mixing length employ an algebraic expression to calculate eddy viscosity, computer time is far less compared to the more advanced closure schemes.

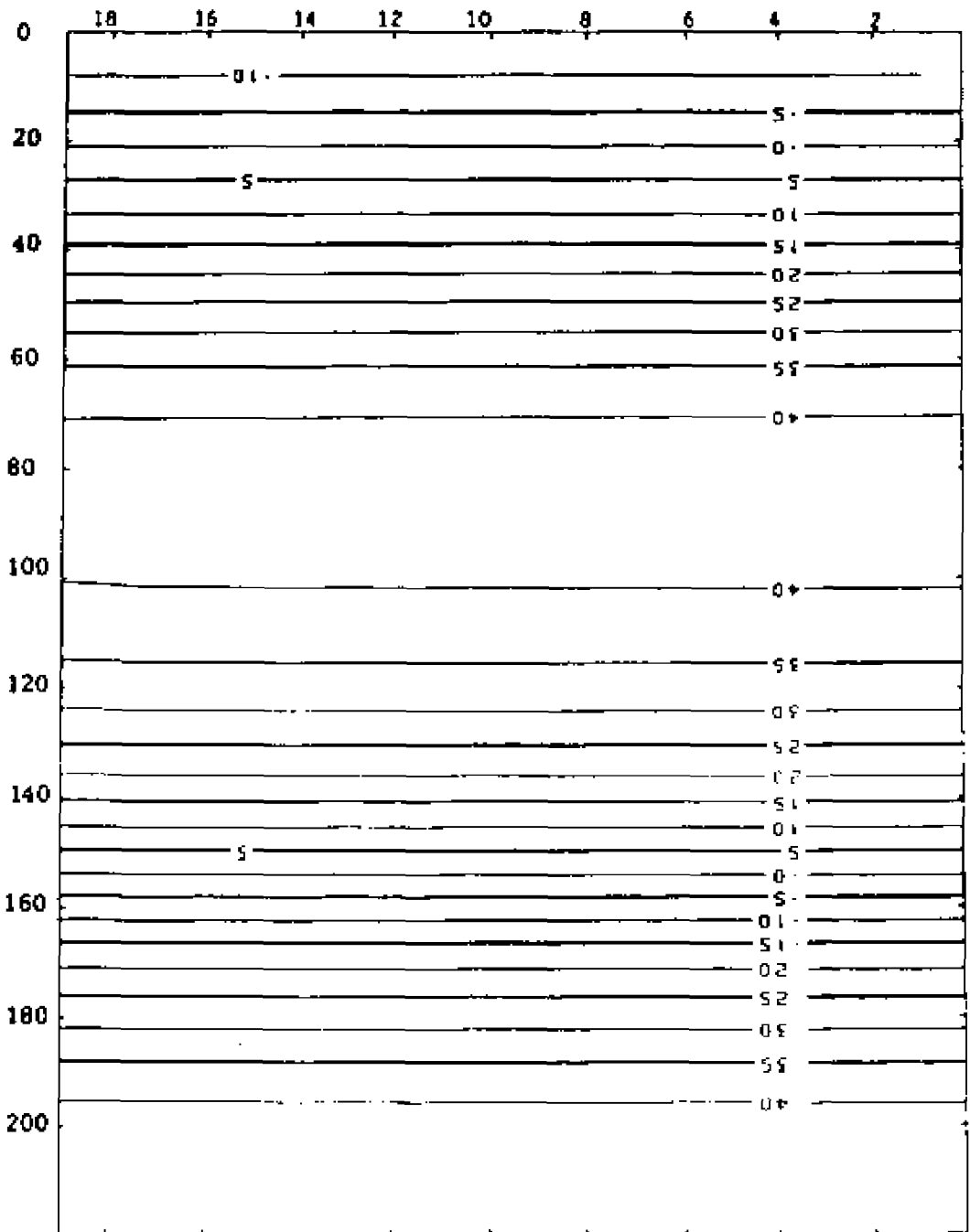
**Table 5-II : Estimates of eddy viscosity, energy and its  
dissipation by level two and mixing length  
models.**

**Table 5.II**

<b>Eq. 4-17</b>	<b>11.4</b>
<b>Level Two Model</b>	<b>18.0</b>
<b>Mixing Length</b>	<b>12.0</b>

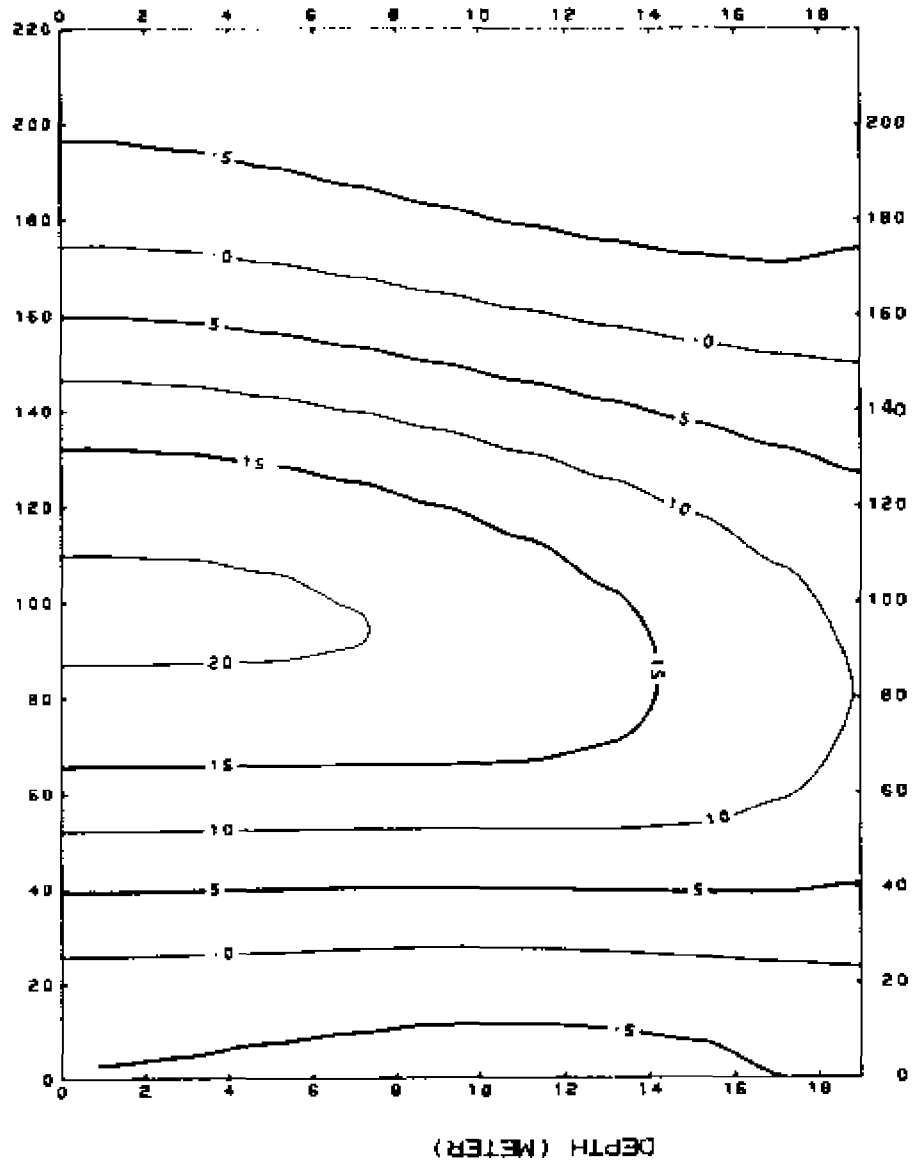
Figure 5.1 : Velocity contours in an open channel; friction forces are not included level two model

DEPTH (METER)



Velocity contours are in cm/sec

Figure 5.2 : Velocity contours in an open channel; friction forces are included level two model



Velocity contours are in cm/sec

Figure 5.3 : Calibration of laboratory bottom roughness level  
two model

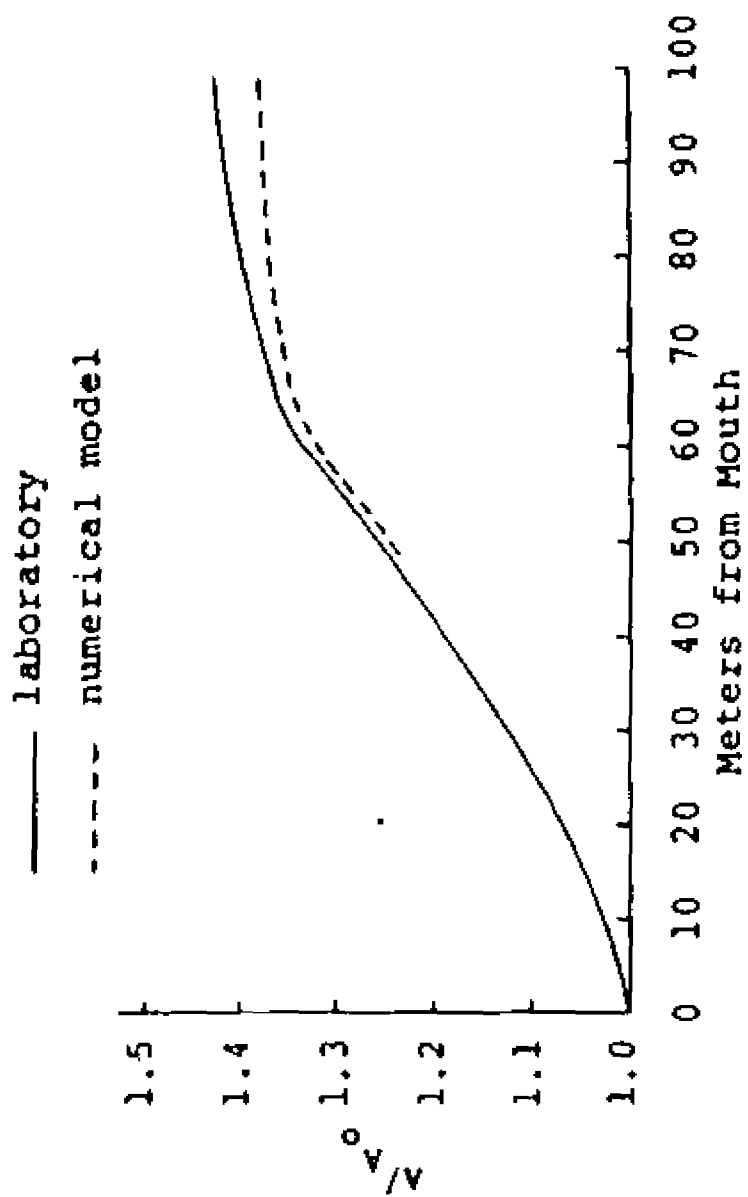


Figure 5.4 : Level two model predictions and flume data of longitudinal salinity distributions and mixing length model predictions

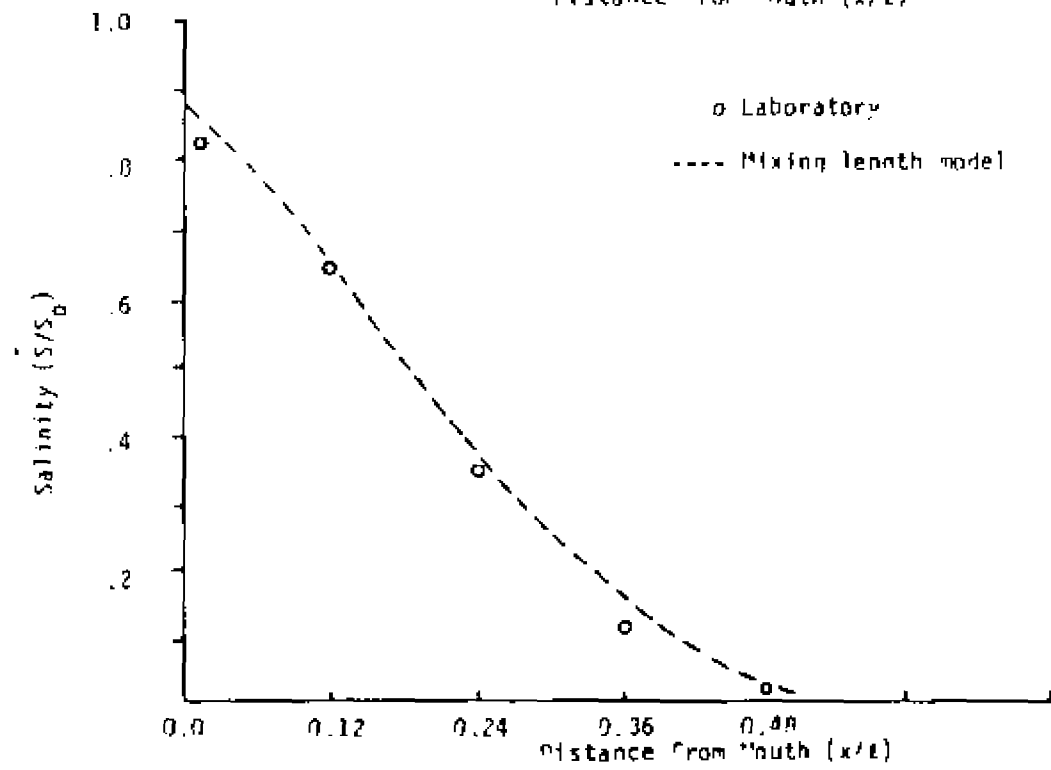
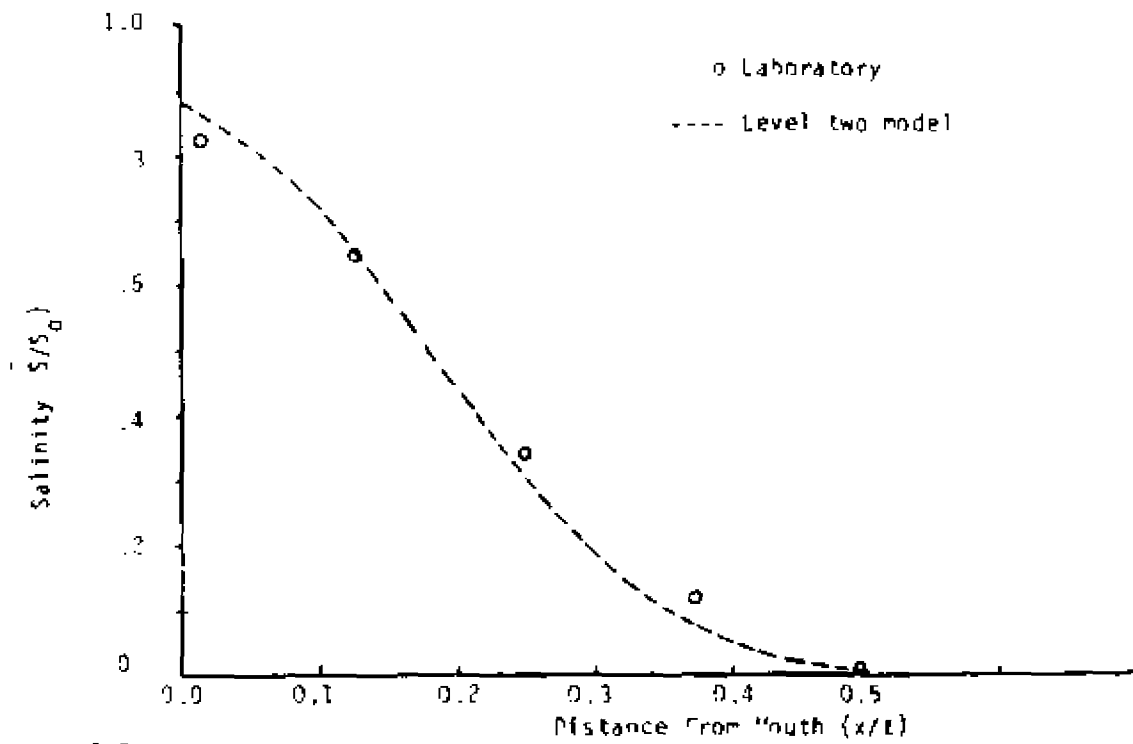
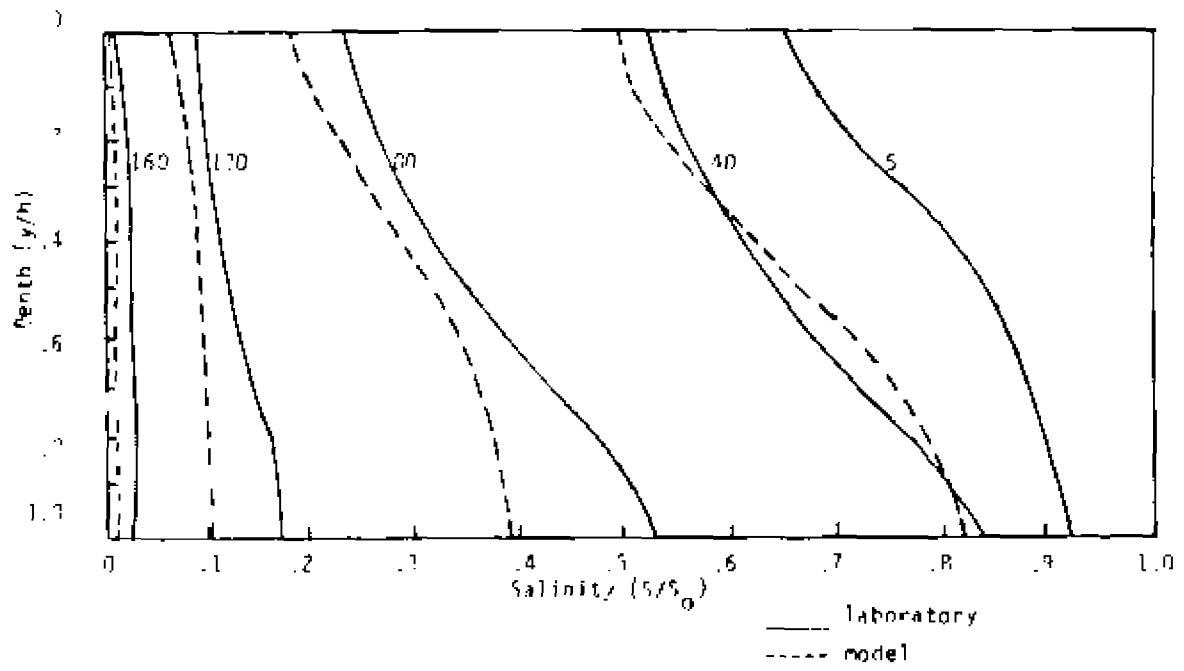


Figure 5.5 : Flume tidal-averaged vertical salinity  
distributions along with the mixing length and  
level two model predictions

Level Two Model



Maximum Length Model

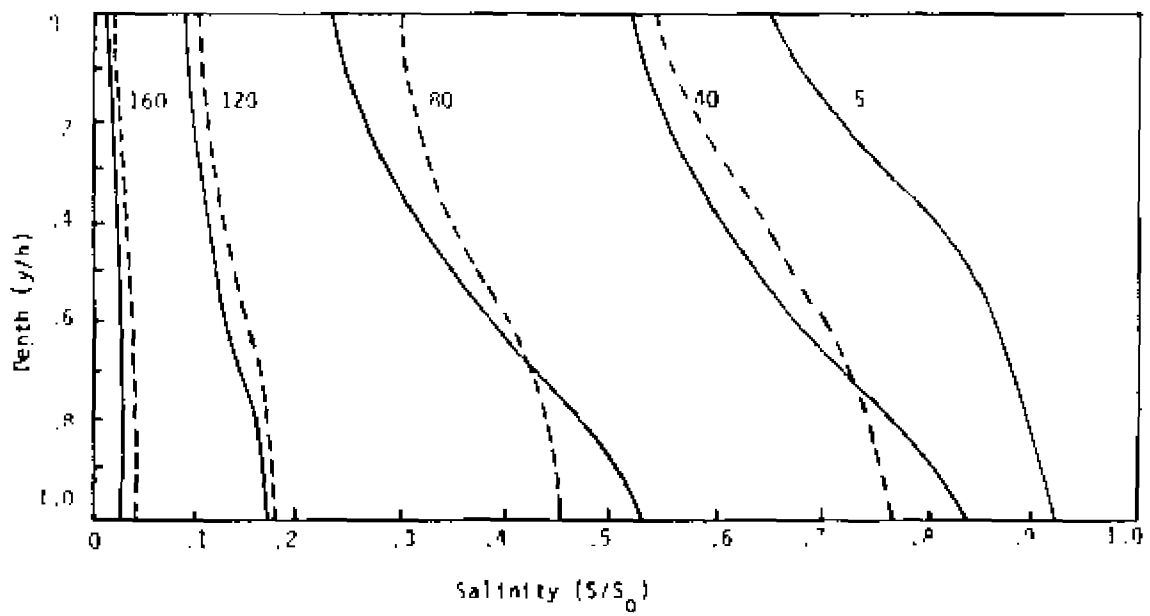
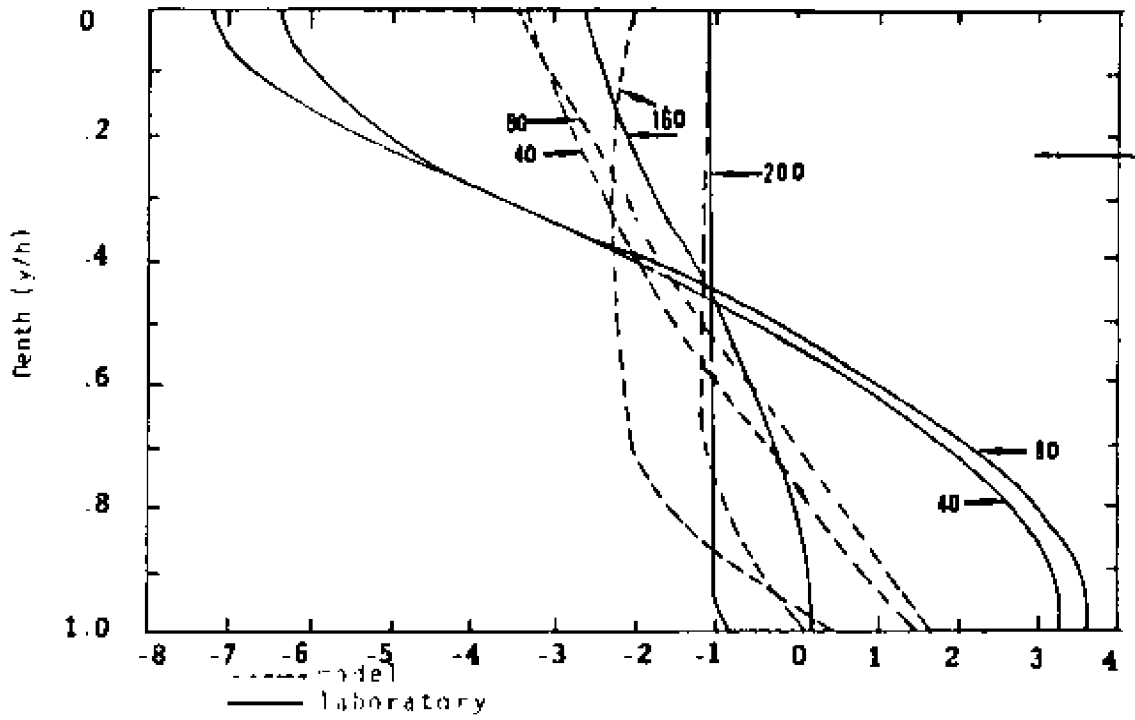


Figure 5.6 : Flume tidal-averaged horizontal velocities along  
with the mixing length and level two model  
predictions

Level Two Model



Mixing Length Model

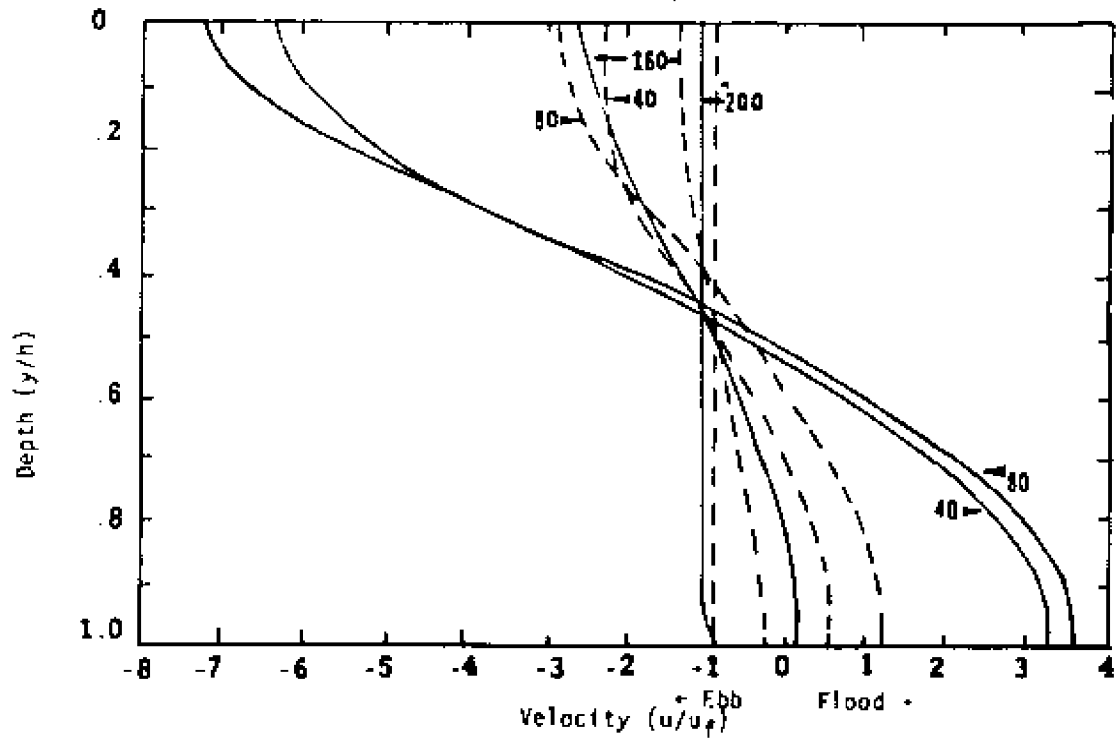
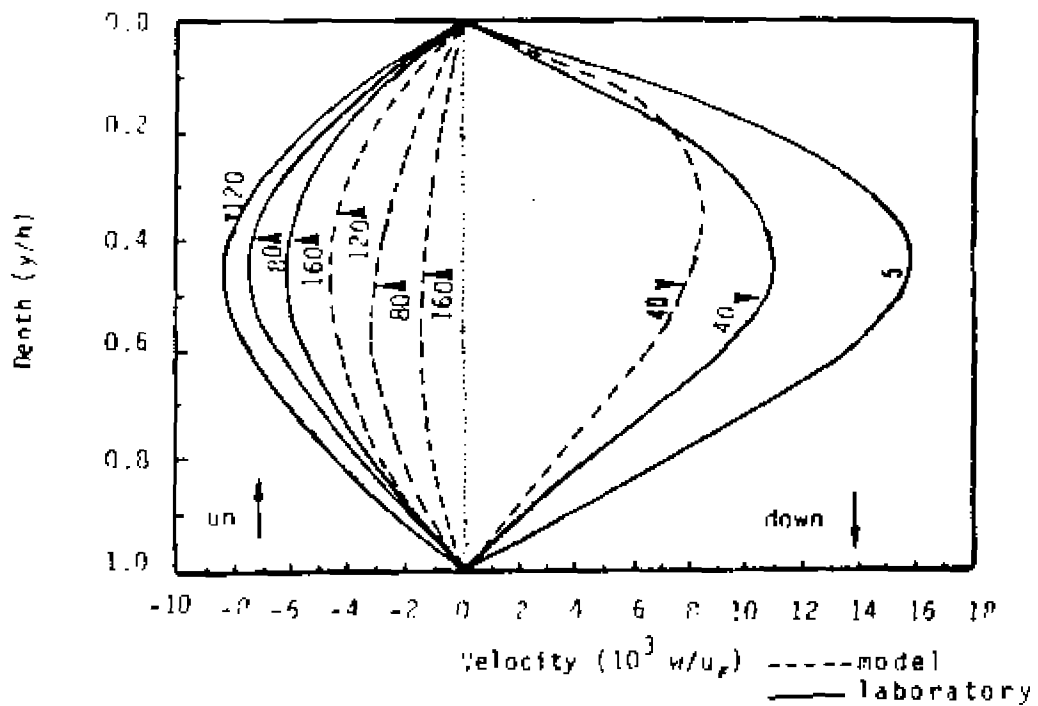
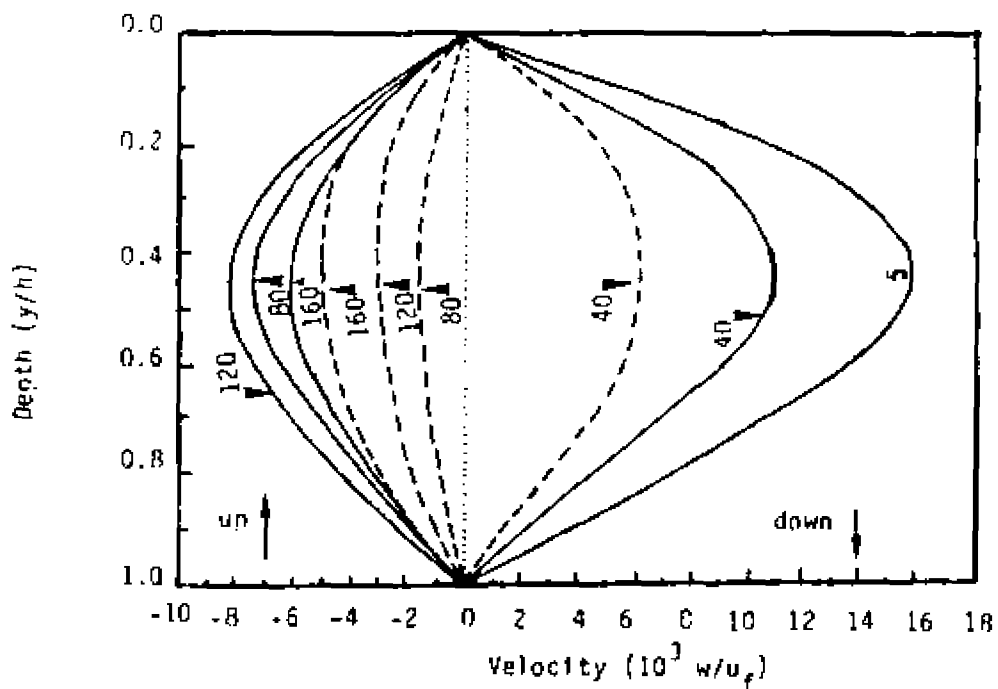


Figure 5.7 : Tidal-averaged vertical velocity distributions;  
flume, mixing length and level two model

Level Two Model



Mixing Length Model



## CHAPTER VI.

### SUMMARY, CONCLUSIONS AND SUGGESTIONS FOR FUTURE WORK

#### Intent of this investigation

The intent of this investigation was to examine two newly proposed turbulence closure schemes: the  $k-\epsilon$  and level two models. Application and comparisons were made between the two new schemes as well as the performance of an existing mixing-length model. Agreement of the models with each other, with analytical solutions, and with experimental data have also been examined. Results obtained from these tests had been compared and discussed in the previous chapter.

This investigation intended to answer the following questions:

- 1- Are the proposed models, either  $k-\epsilon$  or level 2, easier to apply than a mixing-length model ?
- 2- Do the proposed models provide more realistic results than a mixing-length model ?
- 3- Are results improved, if so are the models worthy of pursuing ?

#### A. The $k-\epsilon$ model

In order to answer the first question, one should start with the number of equations employed in each individual model. First of all, the  $k-\epsilon$  model requires solving two partial differential equations (3-14

to 3-15) in addition to the four governing equations. A total of six equations are needed for a solution. This can be translated as an additional burden of greater difficulty and expense in model application. Thus, one can conclude that the k- $\epsilon$  model is not as easy to apply as other models considered in this study. In addition, the time step employed in the numerical scheme for the k- $\epsilon$  model is far less than its counterparts for either closure scheme, i.e. level two or mixing length. The short time step and the additional two equations needed for the closure by the k- $\epsilon$  model, will undoubtedly increase the computational time.

To answer the remaining questions, the k- $\epsilon$  model was tested against a known analytical solution. As stated in Chapter 3, the constant  $C_\mu$  in equation (2-30) must be adjusted in order to achieve agreement with the analytical solution. As can be seen from table 3, better agreement was obtained by employing such a value for  $C_\mu$ . Thus, it is evident that the constant  $C_\mu$  is not as universal as was thought in earlier studies.

As a second test, the k- $\epsilon$  model was applied to a partially mixed estuary. This test was not completed since the buoyancy term can not be reduced as  $R_f$  reached the critical value and hence, the buoyancy term becomes dominant. It is suggested though, that additional attempts to apply this model should be pursued in the future.

The k- $\epsilon$  model in summation :

- A- The k- $\epsilon$  model is more difficult to use and far more computer time is required than with the other two models considered in this study.
- B- The results obtained by the k- $\epsilon$  model are not a substantial improvement compared to the level two or the mixing length models.

C- The constant  $C_\mu$  is not as universal as thought earlier by different authors. For open channel flow, this constant should be set to 0.20 instead of its original proposed value of 0.09.

D- This constant should be expressed as a function of  $R_f$  in order to make the k- $\epsilon$  model applicable to a wide range of flow conditions.

Launder (1976 cited from Rodi, 1980a) has stated that the  $C_\mu$  should be in a functional form rather than a constant as proposed. The suggested constant may take the following form

$$C_\mu = f(R_f)$$

E- The k- $\epsilon$  model is applicable where buoyancy forces have little or no effect, i.e. open channel flow. Agreement for such an application has improved employing the  $C_\mu$  value stated above.

F- The k- $\epsilon$  model does not require an additional expression for the characteristic length scale. The  $\epsilon$  equation solves for a such needed parameter. Thus, one need not specify a different expression for the mixing length scale for various applications as required by other models.

## B. The level two model

Considering the use of the level two model, it is not as complicated as the k- $\epsilon$  model. The level two model does not require the solution of additional partial differential equations but employs a mixing length approach, modified by a stability function, as has been shown in previous chapters. Therefore, one can conclude that the level two model is indeed comparable and as easy to apply as models employing the mixing length hypothesis. Since no additional equations are needed for such a model, the time step used is of the same order as that

employed by the mixing length model. Hence, lengthy model simulations can be performed inexpensively. To summarize the outcome of the level two model:

A- For a homogeneous open channel flow, model predictions of eddy viscosity are in very good agreement with analytical solutions.

B- Model prediction for variables of prime interest are also in very good agreement when compared to data collected under condition where stratification has a pronounced effect on circulation.

C- Constants employed for previous analysis did not require adjustment or tuning throughout the course of this study.

D- The expression used to calculate the characteristic mixing length scale for the level two model is not necessarily adequate for other applications (i.e. jet flows or free jet flows), hence, unlike the k- $\epsilon$  model in which the  $\epsilon$  equation is adequate for most practical applications, an appropriate expression must be selected for the characteristic mixing length for every individual application.

### C. Model comparisons

As a second part of this study, comparisons were made to determine how predictions by the new models compare with the mixing length models. The level two model has shown qualitatively good agreement with analytical solutions. As a second test, the level two model was compared against flume data collected under continually stratified conditions. Agreement, in general, was good and consistent with laboratory data. Results obtained by the level two model are indeed more consistent with flume observations than those of the mixing length model. Level two model results are also an improvement over the mixing

length model when one examines horizontal and vertical velocities. In addition, unlike the mixing length model which requires tuning of the constants with each application, all level two model runs were made with a single set of constants. This is definitely one of the most important outcomes of this study however, more comparisons should be made between model results and observations collected under different flow conditions in order to establish the general applicability of such a model. In conclusion the level two model is definitely an improvement over the mixing length hypothesis and worth pursuing in the future.

#### **D. Suggestion for future investigations**

The intent of this investigation has been achieved. Several difficulties have been encountered during the course of this study. Most difficulties are due to the numerical scheme. The numerical scheme should be such that the time step is infinitely small, which in turn will not allow  $k$  to go to zero. The numerical scheme should also allow for the eddy viscosity to be calculated by using  $k$  and  $\epsilon$  values obtained at the new time step rather than the previous time step.

All equations used in the numerical scheme employed herein require the specification of boundary conditions at channel entrance for their solution. A troublesome task as mentioned earlier, the boundary conditions employed are necessary to solve the equations but they are not necessarily adequate. The results obtained by those conditions should be viewed with caution. A more adequate approach should be pursued such as radiation boundary condition. This approach may improve model predictions in the vicinity of the mouth of a river or estuary.

Results obtained by the level two model are promising. However, more rigorous examination and comparisons with prototype data is recommended.

## BIBLIOGRAPHY

Alfrink, B. J. and Rijn, L. C. Van (1983). **Two-Equation Turbulence Model for Flow in Trenches.** Journal of Hydraulic Engineering, ASCE, Vol. 109, No. 7, July, pp. 941-958.

Blumberg, A. F. (1975). **A Model of Estuarine Circulation.** J. of the Hydraulics Division, ASCE, Vol. 103, pp. 295-309.

Blumberg, A. F. (1975). **A Numerical Investigation into the Dynamics of Estuarine Circulation.** Chesapeake Bay Institute, The Johns Hopkins University. Technical Report 91.

Bowden, K. F. and Hamilton, P. (1975). **Some Experiments with a Numerical Model of Circulation and Mixing in a Tidal Estuary.** Estuarine and Coastal Marine science, Vol. 3, pp. 281-301.

Bradshaw, P. (1972). **The Understanding and Prediction of Turbulent Flow.** Aeronaut. J., Vol. 76, pp. 403-418.

Celik, I. and Rodi, W. (1985). **Calculation of Wave-Induced Turbulent Flows in Estuaries.** Ocean. Engng, Vol. 12, No 6, pp. 531-542.

- Cerco, F. C. (1982). **Two-Dimensional, Intratidal Model Study of Salinity Intrusion Structure and Motion in Partially-Mixed Estuaries.** Dissertation, VA. Inst. of Marine Science, College of William and Mary in Virginia.
- Csanady, G. T. (1964). **Turbulent Diffusion in a Stratified Fluid.** Journal Atmos. Sci, Vol. 31, pp. 439-447.
- Daly, H. J. and Harlow, F. H. (1970). **Transport equations of Turbulence.** Phys. Fluids, vol. 13, pp. 2634-2649.
- Elliott, A. J. (1976). **A Numerical Model of the Internal Circulation in a Branching Estuary.** Chesapeake Bay Institute, The John Hopkins University, Special Report 54.
- Festa, J. F. and Hansen, D. V. (1976). **A Two-Dimensional Numerical Model of Estuarine Circulation: The Effects of Altering Depth and River Discharge.** Estuarine and Coastal Marine Science, Vol. 4, pp. 309-323.
- Fischer, H. B., Imberger, J., List, E. J., Koh, C. Y., and Brooks, N. H. (1979). **Mixing Inland and Coastal Waters.** Academic, Orlando, Fla. pp. 106-107.
- Gibson, M. M. and Launder, B. E. (1978). **Ground Effects on Pressure Fluctuations in the Atmospheric Boundary Layer.** Journal of Fluid Mech., Vol. 86, part 3, pp. 491-511.

Hamilton, P. (1975). **A Numerical Model of the Vertical Circulation of Tidal Estuaries and its Application to the Rotterdam Waterway.** *Geophys. J. R. Astr. Soc.*, Vol. 40, pp. 1-21.

Hansen, D. V. and Rattray, M. R. (1965). **Gravitational Circulation in Straits and Estuaries.** *J. of Marine Research*, Vol. 23, pp. 104-122.

Harleman, D. R. F. and Ippen, A. T. (1967). **Two-Dimensional Aspects of Salinity Intrusion in Estuaries: Analysis of Salinity and Velocity Distributions.** Committee on Tidal Hydraulics, Corps of Engineers, U. S. Army, Tech. Bull. 13.

Henderson, F. M. (1966). **Open Channel Flow.** Macmillan New York, First edn, pp. 98-99.

Hinze, J. O. (1959). **Turbulence An Introduction to Its Mechanism And Theory.** McGraw-Hill Book Company, Inc. New York.

Ippen, A. t. and Harleman, D. R. F. (1961). **One-dimensional Analysis of Salinity Intrusion in Estuaries,** Committee on Tidal Hydraulics, Corps of Engineers, U. S. Army Tech. Bull. 5.

Ippen, A. T. and Harleman, D. R. F. (1966). **Tidal Dynamics in Estuaries,** in *Estuary and Coastal Hydrodynamics*, A. T. Ippen, ed. Engineering Societies Monographs, McGraw Hill Book Co., Inc., New York.

Jabson, H. E. and Sayre, W. W. (1970). **Vertical Transfer in Open Channel Flow.** *Journal of the Hydraulics Division, ASCE*, #43, pp. 703-724.

Kent, R. E. and Pritchard, D. W. (1959). **A Test of Mixing Length Theories in a Coastal Plain Estuary.** *J. of Marine Research*, Vol. 18, pp. 62-72.

Knight, D. W. and Ridgway, M. A. (1976). **An Experimental Investigation of Tidal Phenomena in a Rectangular Estuary.** *International Symposium on Unsteady Flow in Open Channels, BHRA/IAHR, New Castle, Paper B3*, pp. 25-40.

Knight, D. W. (1977). **Velocity Distribution in Unsteady Open Channel Flow with Boundary roughnesses.** *Proc. 17th, IAHR Congress, Baden-baden, F. R. Germany, Paper No. A130, 2*, pp. 437-444.

Kuo, A. Y., Nichols, M. and Lewis, J. (1978). **Modeling Sediment Movement in the Turbidity Maximum of an Estuary.** *Virginia Water Resources Research Center, Blacksburg, Va. Bulletin 111*.

Launder, B. E. and Spalding (1972). **Lectures in Mathematical Models of Turbulence.** Academic Press, London and New York.

Launder, B. E. and Spalding (1974). **The Numerical Computation of Turbulent Flows.** *Computer Methods in Applied Mechanics and Engineering*, Vol. 3, pp. 269-289.

Launder, B. E., Reece, G. J., and Rodi, W. (1975). **Progress in the Development of a Reynolds Stress Turbulence Closure.** *Journal of Fluid Mech.* Vol. 68, pp. 537-566.

Launder, B. E. (1976). **Heat and Mass Transport in Turbulence,** *Topics in Applied Physics*, Vol. 12, Bradshaw, P. ed. Springer-Verlag, New York, pp. 231-287.

Le Mehaute, B. (1976). **An Introduction to Hydrodynamics and Water Waves.** Springer-Verlag, New York, pp. 84-85

Leonard, A. (1974). **Energy Cascade in Large Eddy Simulations of Turbulent Fluid Flows.** *Adv. Geophys.*, Vol. 18A, pp. 237-248.

Mellor, G. L. and Yamada, T. (1974). **A Hierarchy of Turbulence Closure Models for Planetary Layers.** *J. Atmos. Sci.* Vol. 31, pp. 1791-1806.

Mellor, G. L. and Yamada, T. (1982). **Development of a Turbulence Closure Models for Geophysical Fluid Problems.** *Reviews of Geophysics and Space Physics*, Vol. 20, No 4, pp. 851-875.

Oey, L. Y., Mellor, G. L. and Hires, R. I. (1985). **A Three-Dimensional Simulation of the Hudson-Raritan Estuary. Part I: Description of the Model and Model Simulations.** *J. of Physical Oceanography*, Vol. 15, pp. 1676-1692.

Oey, L. Y., Mellor, G. L. and Hires, R. I. (1985). **A Three-Dimensional Simulation of the Hudson-Raritan Estuary. Part II: Comparison with Observation.** *J. of Physical Oceanography*, Vol. 15, pp. 1693-1709.

Oey, L. Y., Mellor, G. L. and Hires, R. I. (1985). **Tidal Modeling of the Hudson-Raritan Estuary.** *Estuarine, Coastal and Shelf Science*, Vol. 20, pp. 511-527.

Pritchard, D. W. (1956). **The Dynamic Structure of A Coastal Plain Estuary.** *J. of Marine Research*, Vol. 15, pp. 33-42.

Pritchard, D. W. (1960). **The Movement and Mixing of Contaminants in Tidal Estuaries.** *Proceeding of the First International Conference on Waste Disposal in the Marine Environment*, ed. E. A. Pearson, Pergamon Press, New York.

Rastogi, A. and Rodi, W. (1978). **Prediction of Heat and Mass Transfer in Open Channels.** *J. of the Hydraulic Division, ASCE*, Vol.

Reynolds, W. C. (1974). **Recent Advances in the Computation of Turbulent Flows.** *Adv. Chem. Eng.* 9 pp. 193-246

Reynolds, W. C. (1976). **Computation of Turbulent Flows.** *Ann. Rev. Fluid. Mech.*, Vol. 8, pp. 183-207

Reynolds, W. C. and Cebeci, T. (1978). **Calculation of Turbulent Flows.** *Topics in Applied Physics*, Vol. 12, pp. 193-229.

Ridgway, M. A. (1975). **An Experimental Study of Tidal Propagation in a Rectangular Estuary. Ph. D. Thesis, University of Birmingham.**

Rodi, W. (1980 a). **Turbulence Models and their Application in Hydraulics - A state of the Art Review. Book Publication of International Association for Hydraulic Research, Delft, Netherlands.**

Rodi, W. (June, 1980 b). **Turbulence Models and Their Applications in Hydraulics. State-of-the-art paper, presented by the IAHR-section on Fundamentals, Division II : experimental and Mathematical Fluid Mechanics.**

Rodi, W. (1985). **Calculation of Flows with a Buoyancy-extended K- $\epsilon$  Turbulence Model, in Turbulence and Diffusion in Stable environment, edit by J. C. R. Hunt. Oxford University Press, New York, pp. 111-143.**

Rodi, W. (1987). **Examples of Calculation Methods for Flow and Mixing in Stratified Fluids. Journal of Geophysical Research, Vol. 92, No. C5, pp. 5305-5328.**

Smith, T. J. and Takhar, H. S. (1979). **On the Calculation of the Width Averaged Flow Due to Long waves in Open Channels. Journal Of Hydraulic Research, Vol. 17, pp. 329-340.**

Smith, T. J. and Takhar H. S. (1981). **A Mathematical Model for Partially Mixed Estuaries Using the Turbulence Energy Equation. Estuarine and Coastal Shelf Science, Vol. 13, pp. 27-45.**

Schlichting, H. (1968). **Boundary Layer Theory**. McGraw-Hill Book Company, Inc. New York.

Tennekes, H. and Lumley, J. L. (1972). **A First Course in Turbulence**. MIT-Press, Cambridge, Mass.

Wang, D. and Kravitz, D. W. (1980). **A semi-Implicit Two-Dimensional Model of Estuarine Circulation**, *J. of Physical Oceanography*, Vol. 10, pp. 441-454.

VITA

Mohamed Zaki Moustafa

Born in Ismailia, Egypt, August 31, 1951. Attended Maadi School (1957-1966) and Maadi High School (1966-1969) in Cairo, Egypt. Obtained a Bachelor Degree in Naval Studies from Egyptian Naval Academy, Alexandria, Egypt, 1973. Obtained a diploma in hydrographic and oceanographic survey from Naval Oceanographic Office, Bay St. Louis, Mississippi, 1980. Received Master of Arts degree from the School of Marine Science, College of William and Mary in 1983. Entered the Doctoral program at the School of Marine Science, College of William and Mary in 1984. Finally found the girl of my dreams, Mary Sue Jablonsky, and tied the knot on November 29, 1986. This work represent the final degree requirement for the Doctor of Philosophy. Employed as a Physical Oceanographer, Technical Resources Inc., Rockville MD, November 1987.